Discovery of a widespread metabolic pathway within and among phenolic xenobiotics

Pahriya Ashrap[a,1], Guomao Zheng[a,1], Yi Wan[a,2], Tong Li[a], Wenxin Hu[a], Wenjuan Li[a], Hong Zhang[a], Zhaobin Zhang[a], and Jianying Hu[a,2]

[a]Laboratory for Earth Surface Processes, College of Urban and Environmental Sciences, Peking University, Beijing 100871, China

Edited by Jerrold Meinwald, Cornell University, Ithaca, NY, and approved May 5, 2017 (received for review January 16, 2017)

Metabolism is an organism's primary defense against xenobiotics, yet it also increases the production of toxic metabolites. It is generally recognized that phenolic xenobiotics, a group of ubiquitous endocrine disruptors, undergo rapid phase II metabolism to generate more water-soluble glucuronide and sulfate conjugates as a detoxification pathway. However, the toxicological effects of the compounds invariably point to the phase I metabolic cytochrome P450 enzymes. Here we show that phenolic xenobiotics undergo an unknown metabolic pathway to form more lipophilic and bioactive products. In a nontargeted screening of the metabolites of a widely used antibacterial ingredient: triclosan (TCS), we identified a metabolic pathway via in vitro incubation with weever, quail, and human microsomes and in vivo exposure in mice, which generated a group of products: TCS-O-TCS. The lipophilic metabolite of TCS was frequently detected in urine samples from the general population, and TCS-O-TCS activated the constitutive androstane receptor with the binding activity about 7.2 times higher than that of the parent compound. The metabolic pathway was mediated mainly by phase I enzymes localized on the microsomes and widely observed in chlorinated phenols, phenols, and hydroxylated aromatics. The pathway was also present in different phenolic xenobiotics and formed groups of unknown pollutants in organisms (e.g., TCS-O-bisphenol A and TCS-O-benzo(*a*)pyrene), thus providing a cross-talk reaction between different phenolic pollutants during metabolic processes in organisms.

triclosan | phenolic xenobiotic | liver microsome | metabolic kinetics | cross-talk reaction

Biotransformation is one of the most important determinants of xenobiotic toxicity in organisms and is becoming increasingly important in environmental toxicology and risk assessment (1, 2). Many xenobiotics that enter the body are lipophilic, and the pollutants undergo biotransformation through the addition of polar groups such as hydroxyls, sugars, and sulfates, which substantially increases the water solubility of the xenobiotics so than they can be more easily excreted (3). Although this process reduces the toxicity of xenobiotics by facilitating their removal from the organism, intermediates may be formed that are much more toxic than the parent compound (1, 4–6). Identification of the bioactive metabolites is essential for assessment of the toxic potential of xenobiotics in organisms.

Phenolic chemicals are an important group of ubiquitous environmental pollutants that include some well-known endocrine disruptors [e.g., triclosan (TCS) and bisphenol A (BPA)] and biotransformation products of aromatic compounds [e.g., hydroxylated benzo(*a*)pyrene (OH-BaP)] (7–9). Phenolic xenobiotics are generally considered to be rapidly detoxified to glucuronide and sulfate conjugates by phase II metabolic enzymes (3), which are often detected in urine, an indication of the normal elimination route in organisms (10, 11). However, the toxicological effects of phenolic chemicals invariably point to their phase I metabolisms. A chronic toxicity study reported that TCS acts as a liver tumor promoter by activating the constitutive androstane receptor (CAR) (8), the regulated genes of which are members of the CYP2B, CYP2C, and CYP3A subfamilies. The metabolism of BPA by liver microsomes can generate more hydrophobic products with higher estrogenic activities (6). These results led us to postulate the existence of active phase I metabolites of phenolic compounds that might contribute to the adverse toxicities in organisms.

To test this hypothesis, we conducted metabolic tests on typical xenobiotics, including chlorinated phenols, phenols, and aromatics. As one of the top 10 aquatic pollutants found in the environment in the United States (12, 13), TCS was the first xenobiotic to be selected for in vitro and in vivo metabolism in diverse species, including fish, bird, rat, and human. Although TCS can be readily detected in biotas (10, 14–17), its biotransformation remains central to the debate over its environmental safety and efficacy in the prevention of food-borne illnesses (18–20). We applied a nontargeted screening strategy to identify a group of TCS biotransformation products that are mainly responsible for CAR activities. The occurrence of the products was confirmed by the investigations of urine samples from the general population. The metabolic pathway was further tested for other xenobiotics in in vitro metabolic systems, and the unknown metabolites were found to be widespread within and among phenolic xenobiotics. The identified metabolic reactions provide a widespread pathway for exploring the potential toxicities and possible cross-talk reactions of phenolic xenobiotics in organisms.

Results

Discovery of an Unknown Metabolic Pathway for TCS.

Identification of the metabolic pathway. Among the target compounds, including chlorinated phenol, phenol, and aromatics, TCS was first selected for in vitro metabolic testing due to its environmental ubiquity and susceptibility to metabolism in organisms. Extracts from the control and TCS-exposed microsomal incubations were analyzed using nontargeted screening strategies

Significance

Organisms are exposed to a wide range of xenobiotics in the environment. Generally, metabolism of individual xenobiotics to water-soluble compounds is a primary defense against these compounds. In this study, we discovered that phenolic xenobiotics undergo a metabolic pathway to form lipophilic ester compounds, and the pathway occurred within and among different compounds in organisms. The pathway provided a mechanism for cross-talk reactions among different pollutants to form groups of unknown compounds during metabolic processes in organisms.

Author contributions: Y.W. designed research; P.A., G.Z., T.L., W.H., W.L., and H.Z. performed research; Y.W. contributed new reagents/analytic tools; P.A., G.Z., Y.W., and Z.Z. analyzed data; and Y.W. and J.H. wrote the paper.

The authors declare no conflict of interest.

This article is a PNAS Direct Submission.

[1]P.A. and G.Z. contributed equally to this work.

[2]To whom correspondence may be addressed. Email: wany@urban.pku.edu.cn or hujy@urban.pku.edu.cn.

This article contains supporting information online at www.pnas.org/lookup/suppl/doi:10.1073/pnas.1700558114/-/DCSupplemental.

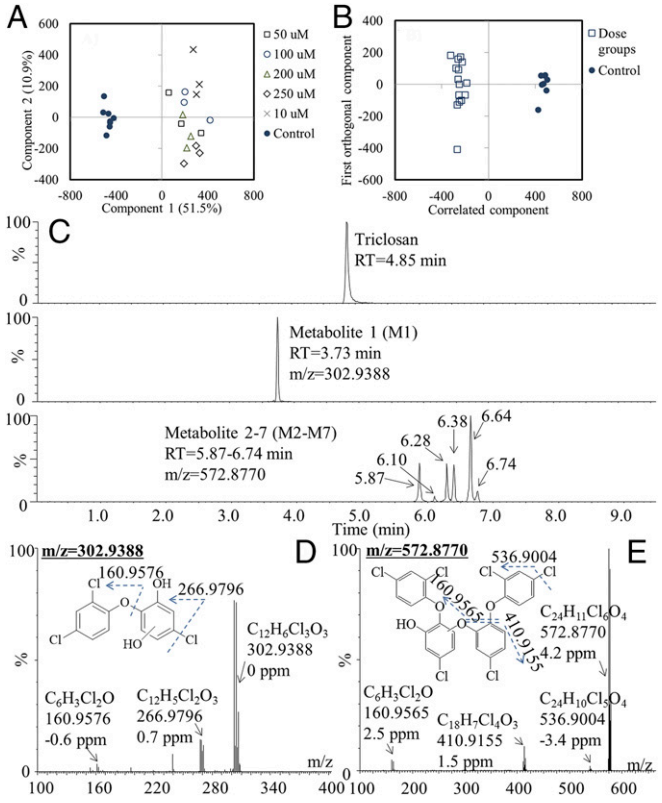

Fig. 1. Identification of metabolites by nontargeted screening. (*A*) PCA score plots of samples from control and dosed groups incubated with human liver microsomes. (*B*) OPLS-DA score plots of samples from the control and dosed groups. (*C*) Chromatogram of TCS and its biotransformation products. (*D*) Mass spectra and proposed structures of metabolite 1. (*E*) Mass spectra and proposed structures of metabolites 2–7.

to identify the potential metabolites. The spectral data of all samples were analyzed by principal component analysis (PCA). Each point in the score plots represents an individual sample, and samples exhibiting similar variances are clustered together. A distinct separation between the control group and the five dosed groups was observed in microsomes of human, quail, and weever (Fig. 1*A* and *SI Appendix*, Fig. S1 *A* and *B*), suggesting that the biotransformation processes resulted in significantly different chemical profiles in the dosed groups compared with the control groups. The discriminatory metabolites that were responsible for class separation were extracted from the S plot of the orthogonal partial least-squares discriminant analysis (OPLS-DA) model of the dosed and control data sets (Fig. 1*B* and *SI Appendix*, Fig. S1 *C* and *D*), and their identities were determined by MS/MS fragmentation. The first groups of metabolites showed the mass spectrum of metabolite 1 (M1) at a retention time of 3.7 min (Fig. 1*C*). On the basis of the molecular ion at *m/z* 302.9388 ($[M\text{-}H]^-$) and the MS/MS fragment ions of 266.9796 ($[M\text{-}H\text{-}Cl]^-$) and 160.9576 ($[M\text{-}H\text{-}C_6H_3ClO_2]^-$), the possible structure was deduced to result from the addition of a hydroxyl to the benzene ring of the TCS (OH-TCS) (Fig. 1*D*). The mass spectrum of another group of metabolites (M2–M7) corresponding to six peaks at 5.87 (M2), 6.10 (M3), 6.28 (M4), 6.38 (M5), 6.64 (M6), and 6.74 min (M7) provided a molecular ion ($[M\text{-}H]^-$) at *m/z* 572.8770 and MS/MS fragment ion at *m/z* 536.9004 ($[M\text{-}H\text{-}Cl]^-$), *m/z* 410.9155 ($[M\text{-}H\text{-}C_6H_4Cl_2O]^-$), and *m/z* 160.9565 ($[M\text{-}H\text{-}C_{18}H_8Cl_4O_3]^-$), as shown in Fig. 1*E* and *SI Appendix*, Fig. S2. One of the TCS-O-TCS isomers (M6) was further chemically synthesized, and the synthesis route and ^{1}H NMR spectrum were shown in *SI Appendix*, Fig. S3. The synthesized compound was eluted as a single peak at the same retention time (6.64 min), and its mass spectrum matched well with that of the compound formed through microsome metabolism (*SI Appendix*, Fig. S4). On the basis of the structural information, TCS formed a group of metabolites, TCS-O-TCS. The pathway existed in all three kinds of microsomes (human, quail, and weever; Fig. 2).

Occurrences in exposed mice and the general population. The above results demonstrate the existence of the metabolic pathway in the in vitro system. We further tested TCS to clarify whether TCS-O-TCS could be formed in in vivo experiments (e.g., mice) and detected in biota samples. Consistent with the results of the in vitro incubations, both OH-TCS and TCS-O-TCS were detected in the livers of mice exposed to TCS for 1 wk (Fig. 3*A*). The concentration ratios of metabolites to the parent compounds (M/P ratio) in the liver tissues of mice were 0.15 and 0.12 for OH-TCS and TCS-O-TCS, respectively. Then a highly sensitive method based on derivatization with dansyl chloride followed by LC-MS/MS was established for the simultaneous analysis of TCS and its biotransformation products in urine samples from the general population (*SI Appendix*, Fig. S5). Among the six TCS-O-TCS metabolites, four compounds (M2, M3, M6, and M7) can be derivertized by separate reactions of the metabolites with dansyl chloride, and two of them (M3 and M6) were detected in the urine samples from a general population (*SI Appendix*, Fig. S5). The structure of the detected predominant metabolite (M6) was clarified by chemically synthesized compound as shown in *SI Appendix*, Fig. S3. OH-TCS was not detected in any of the urine samples, whereas TCS and TCS-O-TCS were detected in 99% and 66% of the samples, respectively (*SI Appendix*, Table S1). The geometric mean urinary concentrations of TCS and total TCS-O-TCS were 11.9 and 0.19 ng/L, respectively (*SI Appendix*, Table S1). The geometric mean of the ratio of TCS-O-TCS to TCS was 0.02 in the general populations. The M/P ratio of TCS-O-TCS found in this study was lower than that of TCS glucuronide but higher than that of TCS sulfate reported previously (10).

Enzyme kinetics. An enzyme kinetic experiment was conducted to further characterize the hepatic microsomal biotransformation of TCS and the formation of metabolites (OH-TCS and TCS-O-TCS) in the three kinds of microsomes (human, quail, and weever). The data on the kinetic properties for the three species fit the classical Michaelis–Menten curve well (*SI Appendix*, Figs. S6 and S7). The biotransformation kinetic parameters (K_m, V_{max}, and K_d) of TCS and the formation kinetic parameters of OH-TCS

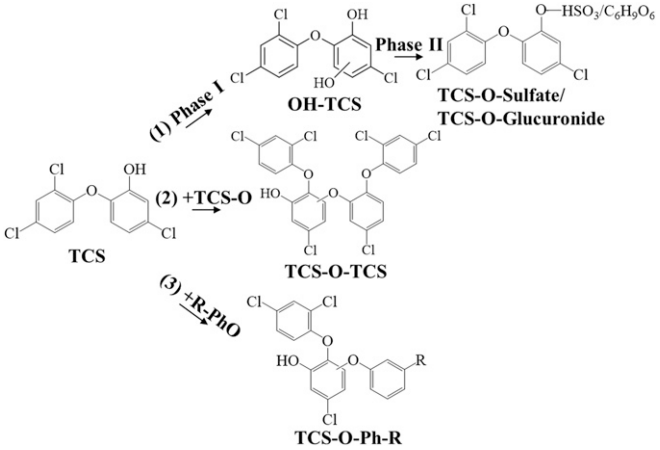

Fig. 2. Metabolic pathways of TCS incubated with liver microsomes. (*1*) Traditional phase I and II metabolism; (*2*) identified metabolic pathway within TCS; and (*3*) identified metabolic pathway among TCS and other phenolic xenobiotics.

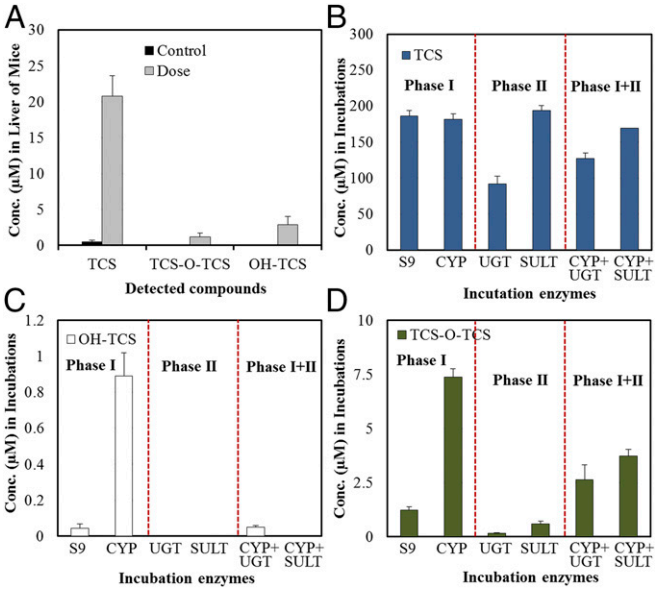

Fig. 3. In vivo and in vitro phase I/II metabolisms of TCS. (*A*) Concentrations of TCS and its biotransformation products in mice liver after exposure to TCS for 1 wk. (*B*) TCS concentrations after incubation with different phase I and II enzymes. (*C*) OH-TCS concentrations after incubation with different phase I and II enzymes. (*D*) TCS-O-TCS concentrations after incubation with different phase I and II enzymes.

and TCS-O-TCS are shown in *SI Appendix*, Table S2. The biotransformation rate of TCS was significantly higher in human microsomes (K_d = 7.0 μL/h/mg protein) and quail microsomes (K_d = 4.2 μL/h/mg protein) than in weever microsomes (K_d = 0.5 μL/h/mg protein). Hydroxylation of TCS (K_d = 3.4–4.5 μL/h/mg protein) occurred at higher rates in human and quail microsomes. TCS-O-TCS was formed at relatively high rates in human microsomes, with K_d values of 0.2–1.2 μL/h/mg protein, followed by quail (0.1–0.4 μL/h/mg protein) and weever (0.1–0.3 μL/h/mg protein).

Phase I and II metabolism of TCS. Reactions were performed with S9, microsome, or cytosolic fractions isolated from human livers. The parent compound TCS was detected at significantly lower concentrations in the cytosolic fraction with the cofactors required for glucuronidation than those in microsome fraction ($P < 0.05$, Fig. 3*B*), which is consistent with the fact that TCS biotransformation is mainly mediated through UDP-glucuronyltransferases (21, 22). Of the incubations with phase I and II enzymes, OH-TCS was only detected in the S9 and microsome fractions with the cofactors required for CYP enzymes (Fig. 3*C*). Significantly larger amounts of TCS-O-TCS were detected in the microsome fractions ($P <$ 0.05) than those in the S9 fraction and cytosolic fractions (Fig. 3*D*). Because the microsome and cytosolic fractions are components of the S9 fraction, the relatively low concentrations of TCS-O-TCS in the cytosolic fractions indicated that the formation of TCS-O-TCS mainly occurred when incubated with microsomes. It should be noted that the incubations with phase II enzymes would have reduced the concentrations of TCS-O-TCS generated by phase I enzymes, but the concentrations of TCS-O-TCS were still higher than those in the S9 and cytosolic fractions (Fig. 3*D*). It is possible that TCS glucuronide or sulfate could act as a reactive intermediate in the formation of TCS-O-TCS. Inhibitors of phase II enzymes were further added to the incubation mixtures. Whereas the concentrations of TCS glucuronide or sulfate were significantly reduced after the addition of the inhibitors, concentrations of TCS-O-TCS were constant in all of the incubations (*SI Appendix*, Fig. S8). The results indicated that TCS glucuronide or sulfate would not act as an intermediate in the formation of TCS-O-TCS, and phase I enzymes mainly catalyze the metabolic reactions.

CAR activities. TCS has been reported to activate the nuclear receptor CAR and substantially accelerate the development of hepatocellular carcinoma, thus acting as a liver tumor promotor (8). In this study, a yeast two-hybrid assay was applied to determine the human CAR binding activities of TCS and its metabolites. This assay has been successfully used to assess the CAR activities of phthalate esters (23). The CAR binding activity potentially stemming from TCS or its metabolites during the biotransformation processes was further evaluated. As shown in Fig. 4*A*, the CAR binding activities of the extracts of TCS incubation mixtures increased with the incubation time, and the concentration to achieve 50% maximal effect (EC_{50}) at 48 h was about 50 times higher than that at 0 h. Chemical analysis showed that TCS concentrations decreased to below the detection limit after 12 h of incubation, OH-TCS concentrations reached stability after 12 h, and TCS-O-TCS concentrations increased with incubation time from 0 to 48 h (Fig. 4*B*). Because no TCS was detected in the incubation mixtures after 12 h, metabolites including OH-TCS and TCS-O-TCS were identified as the compounds that possibly contributed to the CAR binding activities. OH-TCS and TCS-O-TCS were further fractionated to assess their CAR activities. TCS-O-TCS elicited the strongest CAR binding activity followed by OH-TCS and TCS, and the EC_{50} of TCS-O-TCS (0.9 μM) and OH-TCS (2.3 μM) was 7.2 and 2.8 times lower than that of TCS (6.5 μM), respectively (Fig. 4*C*). These results indicate that TCS-O-TCS was the predominant contributor to the CAR activities of the mixtures after 10 h of incubation.

Metabolic Pathway Within Phenolic Xenobiotics. To test whether the identified metabolic reaction is a widespread biotransformation pathway during the metabolism of xenobiotics, the metabolic pathway was further tested in in vitro metabolic systems for other xenobiotics with structures similar to that of TCS. The first group of compounds contained chlorinated phenols [chlorinated BPA (ClBPA) and chlorophenol (ClPhOH)] and had similar structures to that of TCS containing both chlorine and phenols. The second group of compounds included phenols (BPA and PhOH),

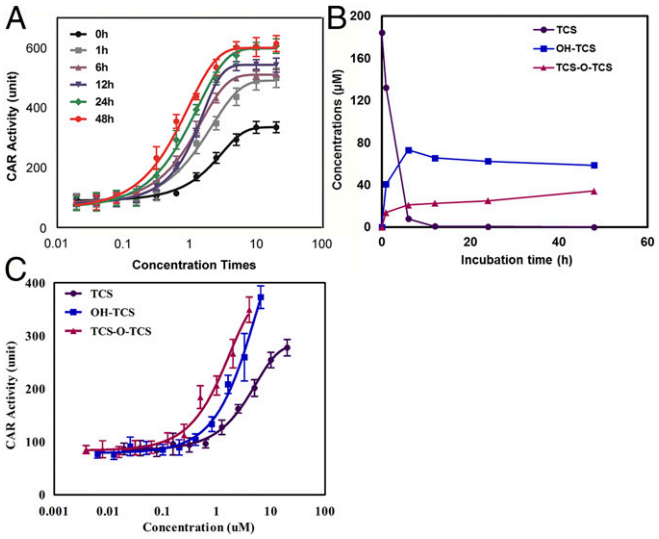

Fig. 4. CAR activities of TCS and its biotransformation products. (*A*) CAR activity of extracts of TCS incubation mixtures at different incubation times. (*B*) Concentration variations of TCS and its biotransformation products at different incubation times. (*C*) CAR activities of TCS and its purified biotransformation products.

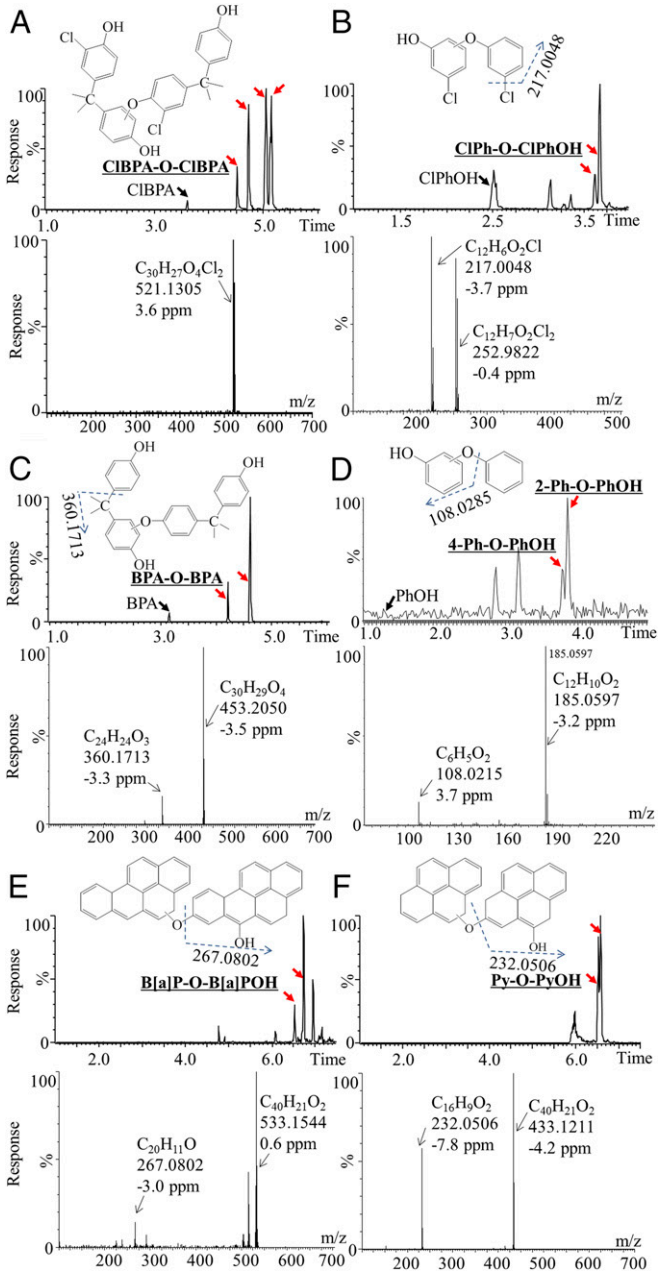

Fig. 5. Chromatogram and mass spectra of the metabolic products: ClBPA (*A*); ClPhOH (*B*); BPA (*C*); PhOH (*D*); B(a)P (*E*); and Py (*F*) after incubation with liver microsomes. Metabolites of Ph-O-PhOH were confirmed with the standards to be 2-Ph-O-PhOH and 4-Ph-O-PhOH.

and their metabolism would test whether chlorine could increase the electronegativity and thus the formation of the products. The third group of compounds comprised aromatics [pyrene (Py), B(a)P, and benzene (Ph)], and their incubation was expected to reveal whether chemicals that contain only benzene could generate the metabolic products. It was interesting to find the generation of metabolites with structures similar to TCS-O-TCS, including ClBPA-O-ClBPA, ClPh-O-ClPh, BPA-O-BPA, and Ph-O-PhOH (Fig. 5 *A–D*). Standards of Ph-O-PhOH were commercially available, including 2-phenoxyphenol (2-Ph-O-PhOH), 3-phenoxyphenol (3-Ph-O-PhOH), and 4-phenoxyphenol (4-Ph-O-PhOH). The detected Ph-O-PhOHs were identified to be 2-Ph-O-PhOH and 4-Ph-O-PhOH, and their liquid chromatogram and quadrupole TOF (QTOF) mass spectra matched well with those of the standards (*SI Appendix*, Fig. S9), and the incubation concentrations of PhOH decreased to 5 μM by using the derivertized GC/MS method for analysis of Ph-O-PhOH. The reaction occurred in the aromatics when their monohydroxylated products formed B(a)P-O-B(a)POH and Py-O-PyOH (Fig. 5 *E* and *F*). These metabolites were more lipophilic than the incubated compounds, as exemplified by their longer retention times on the C18 ultra-performance liquid chromatography (UPLC) column (Fig. 5). The 2-Ph-O-PhOH, 3-Ph-O-PhOH, and 4-Ph-O-PhOH were determined by the derivertized GC/MS method in incubation mixtures with Ph (5–500 μM), because the analytical sensitivities of Ph-O-PhOH is relatively low by UPLC/QTOF/MS analysis. Consistent with the results of PhOH incubations, 2-Ph-O-PhOH and 4-Ph-O-PhOH were detected (*SI Appendix*, Fig. S10), confirming the reaction for the monohydroxylated products of aromatics. By using the derivertized GC/MS method for analysis of B(a)P-O-B(a)POH, and Py-O-PyOH, the incubation concentrations of B(a)P and Py decreased to 5 μM (*SI Appendix*, Figs. S11 and S12). The identified metabolic reaction was a widespread biotransformation process for phenolic compounds (Fig. 2).

Metabolic Pathway Among Phenolic Xenobiotics. TCS was further incubated separately with ClBPA, ClPhOH, BPA, PhOH, Py, and B(a)P to explore whether the metabolic pathway exists among the phenolic xenobiotics. Consistent with the above results, metabolic products including TCS-O-TCS, ClBPA-O-ClBPA, ClPh-O-ClPh, BPA-O-BPA, Ph-O-PhOH, B(a)P-O-B(a)POH, and Py-O-PyOH were detected in the incubation mixtures, confirming the existence of the metabolic pathways within each phenolic compound. We were also surprised to find that compounds such as ClBPA-O-TCS, BPA-O-TCS, B(a)P-O-TCS, and Py-O-TCS were formed when the mixtures were incubated with microsomes, as exemplified by the mass spectra in Fig. 6 *A–D*. No ClPh-O-TCS or Ph-O-TCS signal was found, possibly due to the low responses of the compounds determined by UPLC/QTOF/MS. The detected metabolites also exhibited relatively high lipophilicity compared with the parent compounds. Therefore, the metabolic pathway could also occur among different phenolic chemicals (Fig. 2), providing a cross-talk reaction among different pollutants in organisms.

Discussion

The mass fragmentations of OH-TCS and TCS-O-TCS helped to determine the specific metabolic reaction locations in TCS. As

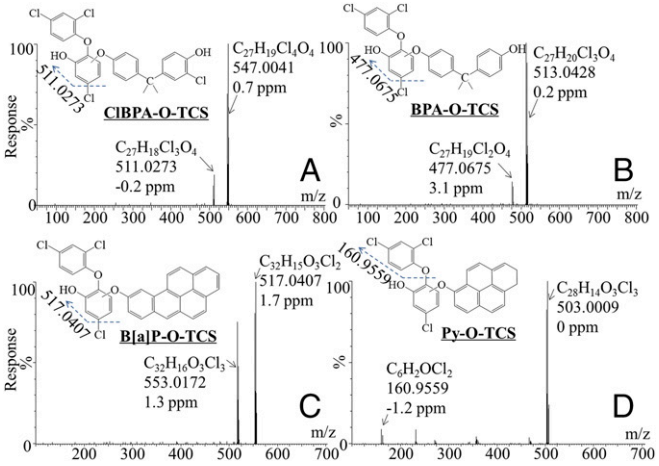

Fig. 6. Mass spectra of the metabolic products among TCS and other phenolic compounds after incubation with liver microsomes. (*A*) ClBPA-O-TCS; (*B*) BPA-O-TCS; (*C*) B(a)P-O-TCS; and (*D*) Py-O-TCS.

shown in Fig. 1 and *SI Appendix*, Fig. S2, the generation of fragment ions ($[M\text{-}H\text{-}C_6H_3ClO_2]^-$) from OH-TCS indicated that the hydroxyl groups were added to the benzene with one chlorine atom in TCS. The generation of fragment ions of $[M\text{-}H\text{-}C_6H_4Cl_2O]^-$ and $[M\text{-}H\text{-}C_{12}H_5Cl_3O_2]^-$ in TCS-O-TCS suggested that a hydrogen ion in the benzene of TCS was substituted by the hydroxyl group of another TCS, and the structure of TCS-O-TCS was confirmed by the chemically synthesized compound (*SI Appendix*, Figs. S3 and S4). Thus, six reaction positions were available for the generation of TCS-O-TCS (Fig. 1*D*), which is consistent with the six TCS-O-TCS isomers detected in the extracts of the dosed incubations. It is interesting to note that no condensation reaction occurred among the TCS hydroxyl groups, and there may have been a loss of H_2O between TCS and OH-TCS, thus forming an ester compound (Fig. 1). The same metabolic pathway was observed within and among the tested phenolic compounds, including chlorinated phenols, phenols, and the monohydroxylated products of aromatics (Figs. 5 and 6). The phenolic xenobiotics produced a group of lipophilic metabolites through this widespread pathway and might exhibit higher biological activities than the parent compounds.

Kinetic studies showed that TCS was rapidly biotransformed in the microsomes of diverse species with a half-life of 0.1–1.4 h (*SI Appendix*, Table S2), which is consistent with the short half-life of TCS in humans (11 h, according to ref. 16). Although a previous study identified phase I metabolites (OH-TCS) in mice after oral administration (24), TCS has been reported to be detoxified mainly through glucuronidation by UDP-glucuronyltransferases (21, 22), and the glucuronide conjugates of TCS were comparable to the total concentrations of TCS in human urine samples (10). A recent long-term exposure study found that TCS promoted liver tumors, and its chronic toxicity was linked to the activation activities of nuclear receptor CAR (8), the regulated genes of which are related to phase I metabolism. In our study, the phase I metabolite TCS-O-TCS was identified after the incubation of TCS with fish, quail, and human microsomes and the exposure of the mice to TCS. The identified metabolites of TCS were consistent with its reported toxicities mediated by phase I metabolic enzymes. The concentrations of TCS-O-TCS continued to increase with the incubation time when TCS was incubated with microsomes for 48 h (Fig. 4*B*). This compound was also detected frequently in urine samples from the general populations. Although the level of TCS-O-TCS was relatively low compared with that of TCS glucuronide in urine samples, the CAR activity of the metabolite was 7.2 times higher than that of TCS. The strong CAR binding activity of TCS-O-TCS was consistent with the high hydrophobicity of the metabolite based on its structure and long retention time on the C18 UPLC column (Fig. 1), as the ligand binding domains of human CAR are primarily hydrophobic (23). Therefore, the highly toxic and persistent metabolite of TCS continuously activated the CAR, although the half-life of parent TCS is very short in organisms. CAR activation regulates genes that are primarily associated with xenobiotic and drug/steroid metabolism (4, 25, 26). Most of the chemical carcinogens are chemically inert and require metabolic activation before they exhibit carcinogenicity in experimental animals and humans (27–29). The above results together indicate that TCS underwent rapid biotransformation to generate active metabolites of TCS-O-TCS, which interfered with the metabolism of other carcinogens via CAR activation and increased the susceptibility of the animals to tumorigenesis.

Phenolic chemicals are an important group of environmental pollutants originating from discharged industrial products (e.g., TCS, BPAs) or the biotransformation of aromatic compounds (e.g., OH-Py) (7–9). Phenolic xenobiotics are generally considered to be rapidly detoxified to glucuronide and sulfate conjugates via phase II metabolic enzymes in organisms (3). Our study reveals that the phase I enzymes mediated an unknown metabolic pathway, which was found to commonly occur within phenolic compounds (Fig. 2). The products generally exhibited higher lipophilic characteristics than the parent compound, suggesting relatively high potential biological activities. Previous studies have reported that the metabolism of phenolic compounds, including BPA, by the liver S9 fraction can generate products with higher estrogenic activities, and the active metabolites exhibited greater hydrophobicity than the parent compound (6). The identified widespread metabolic pathway in this study helps to explain the higher activities of the tested phenolic compounds after their metabolic incubations. Metabolism of B(a)P has been well studied previously (30), and summary of the known metabolic pathways is shown in *SI Appendix*, Fig. S13. It is well known that B(a)P is first oxidized to epoxide intermediates, which are converted with the aid of epoxide hydrolase to diol-epoxides, the ultimate carcinogens (30–34). The epoxide intermediates can also spontaneously rearrange to form phenols or be catalytically hydrolyzed to form dihydrodiols, and are excreted in feces or urine in the form of glucuronide or sulfate conjugates (30, 35, 36). In the present study, B(a)P-O-B(a)P was identified as a metabolite of B(a)P, and this metabolite is different from the reported water-soluble metabolites, exhibiting relatively higher lipophilicities than the parent compound. It is interesting to note that the metabolic pathway also occurred among different phenolic compounds, generating a group of unknown chemicals in organisms (e.g., B(a)P-O-TCS). This provided a pathway for exploring the ecology and health risks of coexposures to different pollutants. TCS is among the top 10 pharmaceuticals and personal care products (PPCPs) in the aquatic environment (12, 18, 20). Most of the PPCPs with high detection frequencies in the environment have phenolic structures (12) and undergo the discovered metabolic pathway in biota. Persistent organic pollutants (POPs) also undergo slow metabolism in organisms to generate phenolic products (e.g., OH-PCBs, OH-PBDEs) (37). The metabolic pathway of TCS revealed in the present study may generalize to PPCPs with susceptibility to the metabolism or coexposure of PPCPs and POPs. The identified metabolic process is also likely to generate more toxic biotransformation products and to provide a cross-talk reaction among different pollutants in the metabolic processes.

In conclusion, this study identified TCS-O-TCS as an unknown biotransformation product of TCS in vitro and in vivo. The metabolites were also frequently detected in the general population, and the CAR activity of TCS-O-TCS was found to be about 7.2 times higher than that of the parent compound. The metabolic pathway was mediated by phase I enzymes and commonly occurred within and among phenolic xenobiotics, thus generating more lipophilic metabolites with potentially high biological activities. The identified metabolic reactions provide a common pathway for exploring the potential toxicities of chemicals with susceptibility to metabolism in organisms, and possible cross-talk reactions among different pollutants.

Materials and Methods

In Vitro Microsomal, S9, and Cytosol Incubations. TCS was incubated with weever, quail, and human microsome incubations to identify the potential metabolites. All incubation experiments were performed in triplicate at 25 °C, 39 °C, and 37 °C for weever, quail, and human microsome incubations, respectively. Incubations with deactivated microsomes (inactivated at 130 °C for 5 min) and standards were used as negative controls. For kinetics studies, hepatic microsomes of the three species were incubated with substrate (TCS, 5, 10, 25, 50, 100, 200, 250, 400, and 500 μM). For metabolic tests within phenolic compounds, hepatic microsomes of the three species were incubated with ClBPA, ClPhOH, BPA, PhOH, B(a)P, Py, and Ph separately. By using UPLC/QTOF/MS and the derivatization GC/MS method for analysis of the identified metabolites, the incubation concentrations of ClBPA, ClPhOH, BPA, PhOH, B(a)P, Py, and Ph were in the range of 10–500, 10–500, 10–500, 5–500, 5–500, 5–500, and 5–500 μM, respectively. In the tests of reactions among phenolic compounds, TCS was incubated with ClBPA, ClPhOH, BPA, PhOH, B(a)P, and Py separately in hepatic microsomes. Concentrations of TCS

were 50 μM in incubations, and concentrations of other reactants were the same as those used in metabolic tests within phenolic compounds. The mass spectra and chromatograms shown in Figs. 1, 5, and 6, and *SI Appendix*, Figs. S9 and S10 were obtained when incubation concentrations of ClBPA, ClPhOH, BPA, PhOH, B(a)P, Py, and Ph were 50, 50, 50, 500, 100, 100, and 50 μM, respectively.

To investigate TCS metabolites produced by phase I and phase II enzymes, TCS was separately incubated with human S9, human liver microsomes, and human liver cytosols. The details of reagents, incubation conditions, chemical analysis, metabolite isolation, CAR assay, data analysis and synthesis route, and NMR analysis of TCS-O-TCS are provided in *SI Appendix*.

Animal Experiments. Animal studies were approved by the Institutional Animal Care and Use Committee of Peking University, and were performed in accordance with the guidelines for animal experiments of the university, which meet the ethical guidelines for experimental animals in China. C57BL/6 mice (6 to 8 wk old) obtained from the Beijing Vital River Laboratory Animal Technology Company were randomly assigned to the treatment and control groups (n = 8). TCS was dissolved in corn oil and administered by gavage at a dose of 100 mg/kg body weight per day. Control received corn oil only. The mice were housed at a temperature of 22 ± 2 °C, a relative humidity of 40–60%, and a 12-h light/dark cycle. The mice were fed a basic diet ad libitum and had access to sufficient drinking water. After 1 wk of TCS treatment, mice were killed, and their livers were removed and subjected to the analysis of metabolites.

Sampling of Human Urines. A scheme devised for the collection of human urine samples was approved by the Human Ethics Committee of Peking University (IRB00001052-12058). A general population comprising 83 adults ranging in age from 24 to 45 y provided urine samples, which were obtained from all participants and poured into individual amber glass tubes. All samples were stored at −20 °C until analysis. We asked each participant to complete a written informed consent form, and with the assistance of qualified public health workers, complete a questionnaire covering information on their lifestyle and social-demographic characteristics: age, sex, body mass index, residence history, smoking habits, and level of education before the sample collection.

Metabolite Identification by Nontargeted Screening. Nontargeted chemical profiling LC/MS analysis was carried out on a Waters ACQUITY UPLC coupled to a Xevo QTOF/MS (G2, Waters) with electrospray ionization as described above. The data of both exposed and control samples from in vitro incubations were analyzed using MarkerLynx software (version 4.1, Waters) with the help of multivariate statistical analysis to reveal any potential metabolites of TCS. The details of the data analysis are provided in *SI Appendix*.

ACKNOWLEDGMENTS. The research was supported by the National Natural Science Foundation of China (21422701, 201677003, and 41330637), the National Basic Research Program of China (2015CB458900), and the Undergraduate Student Research Training Program and the 111 Project (B14001) at Peking University.

1. Gaines TB, Hayes WJ, Jr, Linder RE (1966) Liver metabolism of anticholinesterase compounds in live rats: Relation to toxicity. *Nature* 209:88–89.
2. Cravedi JP (2002) Role of biotransformation in the fate and toxicity of chemicals: Consequences for the assessment of residues in fish. *Revue De Medicine Veterinaire* 153:416–424.
3. Rose RL, Hodgson E (2004) Metabolism of toxicants. *Textbook of Modern Toxicology* (Wiley, New York), ed Hodgson E, 3rd Ed, pp 111–148.
4. Wei P, Zhang J, Egan-Hafley M, Liang S, Moore DD (2000) The nuclear receptor CAR mediates specific xenobiotic induction of drug metabolism. *Nature* 407:920–923.
5. Conney AH (1982) Induction of microsomal enzymes by foreign chemicals and carcinogenesis by polycyclic aromatic hydrocarbons: G. H. A. Clowes Memorial Lecture. *Cancer Res* 42:4875–4917.
6. Yoshihara S, Makishima M, Suzuki N, Ohta S (2001) Metabolic activation of bisphenol A by rat liver S9 fraction. *Toxicol Sci* 62:221–227.
7. Hovander L, Athanasiadou M, Asplund L, Jensen S, Wehler EK (2000) Extraction and cleanup methods for analysis of phenolic and neutral organohalogens in plasma. *J Anal Toxicol* 24:696–703.
8. Yueh MF, et al. (2014) The commonly used antimicrobial additive triclosan is a liver tumor promoter. *Proc Natl Acad Sci USA* 111:17200–17205.
9. Pangrekar J, Kole PL, Honey SA, Kumar S, Sikka HC (2003) Metabolism of chrysene by brown bullhead liver microsomes. *Toxicol Sci* 71:67–73.
10. Arbuckle TE, et al. (2015) Exposure to free and conjugated forms of bisphenol A and triclosan among pregnant women in the MIREC cohort. *Environ Health Perspect* 123: 277–284.
11. Vandenberg LN, et al. (2010) Urinary, circulating, and tissue biomonitoring studies indicate widespread exposure to bisphenol A. *Environ Health Perspect* 118: 1055–1070.
12. Kolpin DW, et al. (2002) Pharmaceuticals, hormones, and other organic wastewater contaminants in U.S. streams, 1999-2000: A national reconnaissance. *Environ Sci Technol* 36:1202–1211.
13. Halden RU, Paull DH (2005) Co-occurrence of triclocarban and triclosan in U.S. water resources. *Environ Sci Technol* 39:1420–1426.
14. Adolfsson-Erici M, Pettersson M, Parkkonen J, Sturve J (2002) Triclosan, a commonly used bactericide found in human milk and in the aquatic environment in Sweden. *Chemosphere* 46:1485–1489.
15. Balmer ME, et al. (2004) Occurrence of methyl triclosan, a transformation product of the bactericide triclosan, in fish from various lakes in Switzerland. *Environ Sci Technol* 38:390–395.
16. Calafat AM, Ye X, Wong LY, Reidy JA, Needham LL (2008) Urinary concentrations of triclosan in the U.S. population: 2003-2004. *Environ Health Perspect* 116:303–307.
17. Pycke B F G, et al. (2014) Human fetal exposure to triclosan and triclocarban in an urban population from Brooklyn, New York. *Environ Sci Technol* 48:8831–8838.
18. Halden RU (2014) On the need and speed of regulating triclosan and triclocarban in the United States. *Environ Sci Technol* 48:3603–3611.
19. DeLeo PC, Sedlak RI (2014) Comment on "On the need and speed of regulating triclosan and triclocarban in the United States". *Environ Sci Technol* 48:11021–11022.
20. Halden RU (2014) Response to Comment on "On the need and speed of regulating triclosan and triclocarban in the United States". *Environ Sci Technol* 48:11023–11024.
21. Moss T, Howes D, Williams FM (2000) Percutaneous penetration and dermal metabolism of triclosan (2,4, 4′-trichloro-2′-hydroxydiphenyl ether). *Food Chem Toxicol* 38: 361–370.
22. James MO, Marth CJ, Rowland-Faux L (2012) Slow O-demethylation of methyl triclosan to triclosan, which is rapidly glucuronidated and sulfonated in channel catfish liver and intestine. *Aquat Toxicol* 124–125:72–82.
23. Zhang H, et al. (2015) Structure-dependent activity of phthalate esters and phthalate monoesters binding to human constitutive androstane receptor. *Chem Res Toxicol* 28: 1196–1204.
24. Wu JL, Liu J, Cai Z (2010) Determination of triclosan metabolites by using in-source fragmentation from high-performance liquid chromatography/negative atmospheric pressure chemical ionization ion trap mass spectrometry. *Rapid Commun Mass Spectrom* 24:1828–1834.
25. Maglich JM, et al. (2003) Identification of a novel human constitutive androstane receptor (CAR) agonist and its use in the identification of CAR target genes. *J Biol Chem* 278:17277–17283.
26. Kawamoto T, et al. (1999) Phenobarbital-responsive nuclear translocation of the receptor CAR in induction of the CYP2B gene. *Mol Cell Biol* 19:6318–6322.
27. Conney AH (2003) Induction of drug-metabolizing enzymes: A path to the discovery of multiple cytochromes P450. *Annu Rev Pharmacol Toxicol* 43:1–30.
28. Guengerich FP (2001) Common and uncommon cytochrome P450 reactions related to metabolism and chemical toxicity. *Chem Res Toxicol* 14:611–650.
29. Shimada T, et al. (1996) Characterization of microsomal cytochrome P450 enzymes involved in the oxidation of xenobiotic chemicals in human fetal liver and adult lungs. *Drug Metab Dispos* 24:515–522.
30. Gelboin HV (1980) Benzo[alpha]pyrene metabolism, activation and carcinogenesis: Role and regulation of mixed-function oxidases and related enzymes. *Physiol Rev* 60: 1107–1166.
31. Yun CH, Shimada T, Guengerich FP (1992) Roles of human liver cytochrome P4502C and 3A enzymes in the 3-hydroxylation of benzo(a)pyrene. *Cancer Res* 52:1868–1874.
32. Shimada T, et al. (1997) Oxidation of xenobiotics by recombinant human cytochrome P450 1B1. *Drug Metab Dispos* 25:617–622.
33. Taura Ki K, et al. (2002) Activation of microsomal epoxide hydrolase by interaction with cytochromes P450: Kinetic analysis of the association and substrate-specific activation of epoxide hydrolase function. *Arch Biochem Biophys* 402:275–280.
34. Chiang HC, Tsou TC (2009) Arsenite enhances the benzo[a]pyrene diol epoxide (BPDE)-induced mutagenesis with no marked effect on repair of BPDE-DNA adducts in human lung cells. *Toxicol In Vitro* 23:897–905.
35. Yang HYL, Namkung MJ, Nelson WL, Juchau MR (1986) Phase II biotransformation of carcinogens/atherogens in cultured aortic tissues and cells. I. Sulfation of 3-hydroxybenzo(a)pyrene. *Drug Metab Dispos* 14:287–292.
36. Fang JL, et al. (2002) Characterization of benzo(a)pyrene-trans-7,8-dihydrodiol glucuronidation by human tissue microsomes and overexpressed UDP-glucuronosyltransferase enzymes. *Cancer Res* 62:1978–1986.
37. Sandau CD, Ayotte P, Dewailly E, Duffe J, Norstrom RJ (2000) Analysis of hydroxylated metabolites of PCBs (OH-PCBs) and other chlorinated phenolic compounds in whole blood from Canadian inuit. *Environ Health Perspect* 108:611–616.

Supporting Information

for

Discovery of a Widespread Metabolic Pathway within and among Phenolic Xenobiotics

Pahriya Ashrap[#], Guomao Zheng[#], Yi Wan*, Tong Li, Wenxin Hu, Wenjuan Li, Hong Zhang, Zhaobin Zhang, Jianying Hu*

Laboratory for Earth Surface Processes, College of Urban and Environmental Sciences, Peking University, Beijing 100871, China

#P.A. and G.Z. contributed equally to this work.

*Address for Correspondence:

Yi WAN, Jianying HU

College of Urban and Environmental Sciences, Peking University

Beijing 100871, China.

TEL & FAX: 86-10-62765520;

Email: wany@urban.pku.edu.cn, hujy@urban.pku.edu.cn.

Chemicals and Reagents.

Triclosan (TCS) and ^{13}C-TCS were purchased from Wellington Laboratories Inc. (Guelph, ON, Canada). Chlorophenol (ClPhOH), phenol (PhOH) and benzene (Ph) were purchased from Dr. Ehrenstorfer GmbH (Germany). Benzo(a)pyrene (B[a]P) and pyrene (Py) was obtained from AccuStandard (New Haven, CT). 2-phenoxyphenol (2-Ph-O-PhOH), 3-phenoxyphenol (3-Ph-O-PhOH), and 4-phenoxyphenol (4-Ph-O-PhOH) were obtained from Ark Pharma Inc. (IL, USA), Alfa Aesar (Ward Hill, MA) and CNW Technologies GmbH (Germany), respectively. BPA was obtained from Kanto Chemical Co. (Tokyo, Japan), and ClBPA was synthesized in our previous study (1). Dichloromethane (DCM), n-hexane, water, acetone, acetonitrile, and methanol of pesticide residue grade were purchased from Fisher Chemicals (NJ, USA). N,O-bis(trimethylsilyl)trifluoroacetamide with 1% trimethylchlorosilane (BSTFA+1% TMCS) was obtained from Supelco (Bellefonte, PA, USA). Dansyl chloride (DNS), 4-(dimethylamino)-pyridine (DMAP), uridine 5'-diphosphate-glucuronic acid trisodium salt (UDPGA), adenosine 3'-phosphate 5'-phosphosulphate (PAPs), dithiothreitol (DTT), 2,6-dichloro-4-nitrophenol (DCNP), and dimethyl sulfoxide (DMSO) were obtained from Sigma-Aldrich (St. Louis, MO, USA). 4-methylumbelliferone (4-MU) was purchased from J&K Technology Limited (Beijing, China). Alamethicin was purchased from TRC (Toronto, ON). Pure water was prepared by a Milli-Q Synthesis water purification system (Millipore, Bedford, MA, USA). The NADPH regenerating system was purchased from Promega (Madison, WI, USA). High performance liquid chromatography (HPLC) grade ammonium acetate was purchased from Dima-Tech Inc. (Richmond Hill, ON, Canada). Sodium sulfate (analytical reagent grade, Beijing Chemicals

(Beijing, China) was baked at 450°C for 4 hours and stored in a drying oven before use. Monopotassium phosphate, dipotassium phosphate, ethylene diamine tetraacetic acid (EDTA), magnesium chloride ($MgCl_2$) and glycerol were purchased from Beijing Chemicals. Human liver microsomes (HLM), human liver cytosols (HLCYT) and human S9 which were pooled (n= 20) from mixed genders, were obtained from BD Biosciences (USA), and stored at -80°C prior to *in vitro* studies. 1,2,4-trichloro-5-nitrobenzene was purchased from TCI organic chemicals. 1,3,5-trimethylbenzene, potassium hydroxide, 4-chloro-2-methoxy-pheno, iron, 1,4-dioxane, hydrochloric acid, sodium nitrite, and boron tribromide were purchased from Adamas Reagent. Cuprous chloride was obtained from Acros chemicals.

Microsome Preparations.

Liver microsome of weever (*Lateolabras japonicus*) and common quails (*Coturnix coturnix*) were prepared according to the method of Dyer et al. (2). HLM, S9, and HLCYT were purchased from the BD biological chemical company (USA) and stored at –80°C before incubation. The weever used in this study was purchased from an aquaculture farm in Qingdao, Shangdong Province, China, and their body weight at the time of use was about 2 kg. Briefly, approximately 5 g of tissue was homogenized in 25 mM phosphate buffer (pH = 7.4, 1.25 mM EDTA, 1mM DTT, 10% (v/v) glycerol), and samples were centrifuged for 15 min at 10,000 × *g*. Following centrifugation, the supernatant (S9 fraction) was removed and then centrifuged at 100,000 × *g* for 60 min. The resulting pellet was dissolved in 10 mL of phosphate buffer (50 mM phosphate buffer, pH = 7.4, 1 mM EDTA, 20% (v/v) glycerol) and stored in liquid nitrogen. Quails were purchased from a farm in Rizhao, Shangdong Province, China and their body weight was about 0.35 kg. Liver microsomes of quail were extracted

according to the method of Diaz et al. (3). Approximately 5 g liver tissue was homogenized in 20 mM phosphate buffer (pH = 7.4, 1 mM EDTA, 250 mM sucrose) and then centrifuged for 30 min at 10,000 × *g*. Following centrifugation, the supernatant (S9 fraction) was removed and then centrifuged at 100,000 × *g* for 90 min. The resulting pellet was dissolved in 10 mL of phosphate buffer (20 mM phosphate buffer, pH = 7.4, 1 mM EDTA, 250 mM sucrose, and 20% (v/v) glycerol) and stored in liquid nitrogen before use. All centrifugation steps were carried out at 4°C, and samples were kept on ice throughout the procedure. The protein concentrations were determined by the Bradford method using bovine serum albumin as a standard according to the manufacturer's protocol (Sigma-Aldrich Corp.) (4).

***In Vitro* Microsomal Incubations.**

For *in vitro* incubations of weever microsomes, reactions were performed in 50 mM phosphate buffer (pH = 7.4) containing 1 mM tetraacetic acid (EDTA), 1 mM dithiothreitol (DTT), and 20% (v/v) glycerol. For *in vitro* incubations of quail microsomes, 50 mM phosphate buffer (pH = 7.4) containing 5 mM $MgCl_2$ and 0.5 mM EDTA were added to the incubation vials. For *in vitro* incubations of human microsomes, the assay was performed in 50 mM phosphate buffer (pH = 7.4) containing 3 mM $MgCl_2$. The reaction mixtures (200 µL), consisting of 100 µL liver microsomes (10 mg/mL protein), 60 µL NADPH regenerating system and 1 uL substrate (TCS dissolved in dimethyl sulfoxide [DMSO]), were incubated in 1.5-mL amber glass vials. After 5 min pre-incubation in a shaking incubator at 25°C, 39°C and 37°C for weever, quail, and human microsomes, respectively, reactions were initiated by the addition of a NADPH-generating system (6.5 mM NADP, 16.5 mM glucose 6-phosphate, 16.5 mM magnesium chloride, and 2 U/mL glucose 6-phosphate dehydrogenase). The protein

concentrations in the incubation mixtures were adjusted to 1 mg/mL. The incubation time was 1 h for kinetic studies, and 12 h for metabolic tests within and among phenolic compounds. After incubations, the reactions were quenched by adding 200 µL of ice-cold acetone. The vials were stored at –20°C until chemical analysis.

***In Vitro* S9 and Cytosol Incubations.**

To investigate TCS metabolites produced by phase I and phase II enzymes, TCS was separately incubated with human S9, HLM, and HLCYT. Incubations of TCS with human S9 were prepared in the microsomes experiments described above using human S9 (2 mg/mL protein) instead of HLM. To investigate TCS metabolites produced by UGT enzymes, reaction mixtures (200 µL) consisting of pooled HLM (1 mg/mL protein), alamethicin (10 µg/mL, 1% DMSO v/v), and TCS were incubated in 1.5-mL amber glass vials. The reaction was initiated by the addition of 1mM trisodium salt (UDPGA). A new aliquot of UDPGA was added after 9 h incubation to ensure a sufficient cofactor amount throughout the experiment. To investigate TCS metabolites produced by SULT enzymes, samples were prepared as described above for the UGT experiments without the addition of alamethicin, using 1 mg/mL HLCYT instead of HLM and starting the reaction by the addition of 0.1 mM adenosine 3’-phosphate 5’-phosphosulphate (PAPs) instead of UDPGA. Phase II enzyme inhibition experiments were conducted by adding enzyme inhibitors to the incubation mixtures described above. 2,6-dichloro-4-nitrophenol (DCNP) and 4-methylumbelliferone (4-MU) were inhibitors of UGT and SULT enzymes in HLM, respectively, and the inhibitors were added using the corresponding reaction buffer as the solvent.

All reactions were performed in triplicate at 37°C and quenched after 18 h by adding 200 μL acetone. The vials were stored at −20°C until chemical analysis. Incubations with deactivated enzymes and standards were used as negative controls to assess potential background interference and the possibility of non-enzymatic changes.

Analysis of Incubation Mixtures.

For analysis of TCS incubation mixtures, the mixtures were spiked with 100 μg internal standards (^{13}C-TCS) and extracted with 1 mL hexane three times. The aquatic fraction was then passed through a Pasteur pipe filled with sodium sulfate to remove moisture and then eluted by 2 mL hexane and 2 mL DCM, which were also used to rinse the glass vial before elution. All of the extracts were combined and concentrated to 200 μL in hexane for instrumental analysis. An aliquot of extract (100 μL) was derivatized with BSTFA+1% TMCS for analysis of TCS. Briefly, 100 μL BSTFA+1% TMCS was added into the vial containing the extracts, which was dried under a gentle stream of nitrogen gas before the derivatization. The mixture was allowed to react for 1 h at 70°C. After cooling for 5 min, the final sample volume was adjusted to 100 μL using hexane for gas chromatography–mass spectrometry (GC-MS) analysis. The remaining 100 μL of extract was reconstituted with 100 μL of methanol for the untargeted screening of biotransformation products by ultrahigh-pressure liquid chromatography (UPLC) coupled to a quadrupole time-of-flight mass spectrometer (QTOF-MS). For analysis of incubation mixtures of ClBPA, ClPhOH, BPA, PhOH, B[a]P, and Py, the extraction procedures were same to those of TCS and the extracts were directly reconstituted with 100 μL of methanol for UPLC-QTOF-MS analysis. For analysis of incubation mixtures of Ph, the extracts were derivatized with BSTFA+1%

TMCS for GC-MS analysis.

Analysis of Rat Liver and Urine Samples.

Approximately 1 g of tissue was homogenized in 1 mL ultrapure water, spiked with 100 μg internal standard (^{13}C-TCS), and then extracted with 2 mL hexane three times. The aquatic fraction was then passed through sodium sulfate to remove any moisture and eluted by hexane and DCM. All of the extracts were combined and concentrated to 50 μL for dansylation before UPLC-MS/MS analysis. Human urine samples (25 mL) were acidified with 0.1 M formic acid, ^{13}C-TCS was added to obtain a final concentration of 5 ng/L, and then the samples were extracted with 25 mL hexane two times and 25 mL (hexane: DCM = 3: 1). The extract was dried and dissolved in 1 mL acetonitrile for dansylation. Dansylation was applied to improve the analytical sensitivities of TCS and its biotransformation products. Briefly, 200 μL of 30 mg/mL dansyl chloride and DMAP in DCM was added to the extract solution. The mixture solution was shaken vigorously for 1 min. The resulting mixture was kept at 65°C for 60 min and then extracted with 2 mL hexane three times. The extract was evaporated to dryness and reconstituted with 25 μL of methanol prior to UPLC-MS/MS analysis.

GC-MS Analysis.

Sample analyses were performed with an Agilent 6890 equipped with a 5975C mass spectrometer (Agilent Technologies) in EI (electron impact) mode. Analytes were separated on a HP-5ms column (30 cm × 0.25 mm × 0.25 μm film thickness; J&W Scientific) with helium as the carrier gas (1.0 mL/min). The oven temperature program was 80°C for 1 min, 30°C/min to 180°C, 5°C/min to 260°C, 20°C/min to 300°C, and then 300°C for 10 min. The ion source temperature was maintained at 250°C and the electron energy was 70 eV. Sample

(1 μL) was injected into the GC-MS system in splitless mode, and the injector was held at 280°C. The following masses were used for confirmation and quantification of TCS: m/z = 345, 347, and 200 for the derivative of TCS, m/z = 357, 359, and 200 for internal standard ^{13}C-TCS, m/z =258, and 243 for the derivatives of Ph-O-PhOH, m/z =526, and 453 for the derivatives of for Py-O-PyOH, and m/z=626, and 285 for the derivatives of for B[a]P-O-B[a]POH.

UPLC-QTOF-MS Analysis.

Analysis was performed on an ACQUITY^{TM} UPLC system (Waters, Milford, MA, USA) coupled to a Xevo QTOF-MS (G2, Waters) equipped with an electrospray ionization source. Instrument control was performed using MassLynx Software (Waters, software version V4.1). UPLC separation was achieved using a Waters ACQUITY^{TM} UPLC BEH C8 column (50 × 2.1 mm, 1.7-μm particle size). The column was maintained at 60°C at a flow rate of 0.6 mL min^{-1} and the injection volume was 3 μL. The mobile phases consisting of ultrapure water containing 5 mM ammonium acetate and 0.05% acetic acid (A) and acetonitrile (B) were used with gradient elution. The gradient applied was as follows: 0 min, 5% B; 7 min, 95% B; 8 min, 95% B; 8.1 min, 5% B; and 10 min, 5% B. The mass spectra were acquired in the negative ion mode. The analysis was performed in full scan mode in the mass range of 80-700 Da with a 1-s scan time. The optimized parameters were as follows: source capillary voltage, -0.7 kV; sampling cone voltage, 35 V; extraction cone voltage, 4.0V; source temperature, 100°C; cone gas flow rate, 50 L/h; and desolvation gas flow rate, 950 L/h. Nitrogen and argon were used as cone and collision gases, respectively. The [M-H]$^-$ ion of leucine-enkephalin (200 pg/μL infused at 5 μL/min) was used as a reference lock mass (m/z = 554.2615). The QTOF detector

was calibrated with a sodium formate solution to achieve a mass accuracy below 3 ppm by using leucine-enkephalin as the lock mass in negative mode. The accuracy of mass measurement in combination with the retention times in UPLC was used to calculate empirical formulae for TCS. For MS/MS analysis, the experimental conditions were the same as above except for the collision energy. Three levels of collision energy were applied: 5~15V, 15~25V, and 25~35V.

UPLC-MS/MS analysis.

The LC apparatus was an ACQUITY^{TM} Ultra Performance LC system (Waters). Separations were conducted using a Waters ACQUITY^{TM} UPLC BEH C8 column (50 × 2.1 mm, 1.7-μm particle size). The column was maintained at 40°C, and the flow rate and injection volume were 0.6 mL/min and 5 μL, respectively. Ultrapure water containing 0.1% formic acid (A) and acetonitrile (B) were chosen as the mobile phases. The gradient applied was as follows: 0 min, 5%B; 7 min, 95% B; 8 min, 95% B; 8.1 min, 5% B; and 10 min, 5% B. The optimized parameters were as follows: source temperature, 110°C; desolvation temperature, 350°C; capillary voltage, 3.50 kV; desolvation gasflow, 800 L/h; cone gas flow, 50 L/h; and multiplier, 650 V. The mass spectra were acquired in the positive ion mode. Data acquisition was performed by multiple reaction monitoring (MRM). The optimized MRM transitions, cone voltages, and collision energies were summarized in the Table S3.

Separate Isolation of Metabolites.

Preparative HPLC was performed to isolate the individual metabolites (e.g. individual TCS-O-TCS isomers) with a Shimadzu high performance liquid chromatography system (LC-20AT) equipped with a UV detector (SPD-20A), using an YMC C18 preparative column

(5 μm particle size, 250 mm x 10 mm i.d.). The processing conditions for the gradient elution were as follows: 0-2 min, acetonitrile-water (5:95, v/v); 2-52 min, acetonitrile-water (100:0, v/v); 52-60.5 min, acetonitrile-water (5:95, v/v); 60.5-66 min, acetonitrile-water (5:95, v/v). The flow rate was 4.5 mL/min. The target fractions were collected, confirmed by UPLC-QTOF-MS analysis.

Statistical analysis of Nontargeted Screening.

Spectral peaks were deconvoluted and aligned using Waters MarkerLynx with the following parameters: initial retention time of 1 min, final retention time of 8 min, and mass in the range 50–1200 Da, with a mass tolerance of 0.02 Da, mass window of 0.02 Da, retention time window of 0.2 min, and noise elimination level 6. For peak integration, the peak width at 5% of the height was 1 s, the peak-to-peak baseline noise was automatically calculated, and the peak intensity threshold was 100. No specific mass or adduct was excluded. Isotopic peaks were excluded for analysis. The data sets were exported to SIMCA-P+ (ver. 12.0, Umetrics, Umea, Sweden) for multivariate statistical analysis. Principal component analysis (PCA) and orthogonal partial least-squares-discriminant analysis (OPLS-DA) were conducted to identify the discriminatory chemicals based on the comparison of exposed and control samples. The accurate mass composition and fragmentation pattern of each marker feature of interest (as determined by multivariate techniques) were further determined by UPLC-QTOF-MS/MS analysis.

Quality Assurance and Quality Control (QA/QC).

All equipment was rinsed with acetone and hexane to avoid sample contamination. Procedural blanks were prepared with Milli-Q water to determine background contaminations.

Concentrations of TCS and TCS-O-TCS in sample extracts were quantified relative to ^{13}C-TCS. Efficiencies of the sample preparation procedures for urine samples were assessed by analyzing samples spiked with standard solutions of TCS and purified standards of TCS-O-TCS and OH-TCS. The absolute recoveries of target compounds in triplicate spiked samples were 72 ± 11%. Surrogate standards were spiked to samples prior to extraction to compensate for the loss of target compounds during the extraction process and correct the variation of instrument response and matrix effect. The recoveries of ^{13}C-TCS were 85 ± 13% in all of the sample analyses. Instrumental method detection limits for TCS on GC-MS were both below 0.3 μg/mL and were 0.03, 0.02, and 0.01 ng/mL for TCS, OH-TCS, and TCS-O-TCS, respectively, on UPLC-MS/MS.

Chemical Synthesis of a TCS-O-TCS isomer.

As shown in SI Appendix, Fig. S3, a solution of compound B (1.0 eq) and KOH (1.0 eq) in mesitylene was heated to 150°C for 30 min, then a solution of compound A (1.0 eq) was added into the solution, and stirred at this temperature for 16 hours, then the mixture was concentrated and purified by Prep-TLC to give compound C (400 mg, 50%) as a yellow treacly appearance. A solution of compound D (1.0 eq) and KOH (1.0 eq) in mesitylene was heated to 150°C for 30 min, then a solution of compound C (1.0 eq) was added into the solution, and stirred at this temperature for 16 hours, then the mixture was concentrated and purified by Prep-TLC to give compound E (20 mg, 20%) as a white solid. A solution of compound E (1.0 eq) in H_2O/dioxane=1/1 was added with Fe (10 eq) and 3 drops of conc.HC. This mixture was heated at 100°C for 3 hours, and then filtered, concentrated, and purified by Prep-TLC to give compound F (10 mg, 45%) as a yellow oil. A solution of compound F (1.0

eq) in H_2O/conc.HCl=1/1 was added with $NaNO_2$ (1.5 eq) at 0°C and stirred for 30 mins, then $CuCl_2$ (2.0 eq) was added into the solution, warmed to room temperature, and stirred for 3 hours. Then the solution was extracted by DCM, dried over Na_2SO_4, filtered and concentered to give compound G (8.0 mg) as a crude material. A solution of compound G (1.0 eq) in DCM was cooled to -78°C and then BBr_3 (3.0 eq) was added into the solution, warmed to room temperature for 3 hours, then 2 mL MeOH was added into the solution, concentrated and purified by Prep-TLC to give product (1.2 mg) as a light red solid.

The synthesized substance was dissolved in 600 μL chloroform-d, and used for ^1H nuclear magnetic resonance (NMR) analysis. ^1H NMR spectra were recorded at 500 MHz on a Bruker AVANCE III 500 spectrometer. The substance was also redissolved in methanol for UPLC-QTOF-MS analysis.

CAR Activation Assay.

The yeast two-hybrid assay was used to test the binding activity of TCS and its metabolites with the CAR. This system is based on the ligand-dependent interaction of two proteins, a human CAR and a coactivator transcriptional intermediary factor 2. The extracts of the incubation mixtures or isolated metabolites were treated with yeast cells to determine their CAR activities. The microsomes and NADPH system were re-added to the incubation mixtures every 12 h to supplement the protein. The yeast cells were pre-incubated overnight at 30°C (about 14-16 h) with vigorous shaking in 5 mL SD medium (6.7 g/L Difco yeast nitrogen base without amino acids, 2% glucose, 300 mg/L L-isoleucine, 1,500 mg/L L-valine, 200 mg/L L-adenine hemisulfate salt, 200 mg/L L-arginine HCl, 200 mg/L L-histidine HCl monohydrate, 300 mg/L L-lysine HCl, 200 mg/L L-methionine, 500 mg/L L-phenylalanine,

200 mg/L L-threonine, 300 mg/L L-tyrosine, and 200 mg/L L-uracil [Sigma-Aldrich]) until the cell density reached an optical density (OD) level of 0.4. The OD levels were measured by a microplate reader (Bio RAD 550, Richmond, CA, USA) operating at a wavelength of 595 nm. Cell cultures (50 μL) and 2.5 μL TCS standards or extracts of incubations dissolved in DMSO solution were then added to 200 μL fresh medium, respectively. After incubation at 30°C for 4 h, 150-μL aliquots of the culture mixtures were removed to determine the absorbance at 595 nm. The residual culture was centrifuged (12,000 rpm) for 5 min at 4°C, and the collected cells were digested enzymatically by resuspension in 200 μL Z buffer (0.1 M sodium phosphate, 10 mM KCl, and 1 mM $MgSO_4$) containing 1 mg/mL Zymolyase 20T (Seikagaku, Tokyo, Japan) at 30°C for 20 min. The lysate was mixed with 40 μL 4 mg/mL 2-nitrophenyl-b-D-galactoside (ONPG, Tokyo Kasei, Tokyo, Japan) at 30°C and reacted until the development of a yellow color (usually 20 min). Then, 100 μL 1 M Na_2CO_3 was added to finalize the enzymatic reaction and 150-μL aliquots were added into each well in a 96-well microplate. Absorbances at 415 and 570 nm were read on the microplate reader, and based on the absorbances at 595, 415, and 570 nm, CAR activity was calculated by the following equation:

$$U = 1{,}000 \times ([OD_{415}] - [1.75 \times OD_{570}]) / ([v] \times t \times [OD_{595}]),$$

where U = CAR activity, t = time of reaction (min), v = volume of culture used in the assay (ml), observed density $(OD)_{595}$ = cell density at the start of the assay, OD_{415} = absorbance by o-nitrophenol at the end of the reaction, and OD_{570} = light scattering at the end of the reaction. CITCO, a human CAR selective agonist, was used as a positive control. Stock solutions of test chemicals were subjected to a 2-fold serial dilution with DMSO to prepare 11

concentrations in the range of 9.77×10^{-2} to 100 μM. All results are given as the mean ± standard deviation (SD) of at least triplicate assays. The REC50 is the concentration of the test chemical corresponding to 50% of the maximum activity of TCS. Sigmoidal dose-effect curves for human CAR binding activities were analyzed using GraphPad Prism 5 Software (GraphPad Software, Inc., San Diego, CA).

Data Analysis.

After the Pareto scaling (mean centering and scaling to the square root of variance), the data sets were exported to SIMCA-P 13.0 (Umetrics) for multivariate statistical analysis including PCA and OPLS-DA analysis. Each OPLS-DA model was evaluated by both the internal permutation test and external validation test. Unpaired Student's *t*-tests, with a Bonferronni correction for multiple comparisons, were used to ensure that the markers extracted with holistic OPLS-DA analysis were significantly differentially expressed between the exposed and control groups. A *p*-value threshold of 0.05 was used to define significance. Enzyme kinetic data were fit to the Michaelis-Menten model using GraphPad Prism 5 Software (GraphPad Software, Inc.).

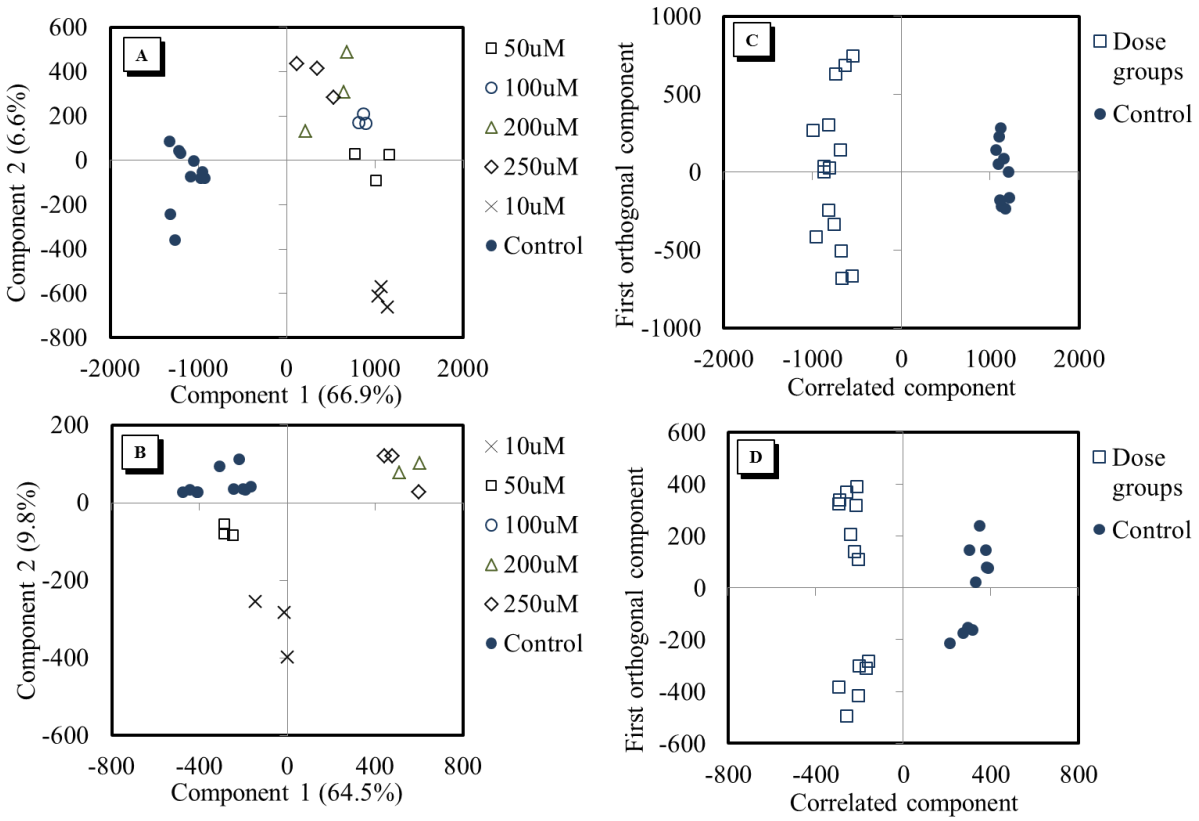

Fig. S1. A) PCA score plots of samples from control and dosed groups incubated with quail microsomes; B) OPLS-DA score plots of samples from control and dosed groups incubated with quail microsomes; C) PCA score plots of samples from control and dosed groups incubated with weever microsomes; D) OPLS-DA score plots of samples from control and dosed groups incubated with weever microsomes

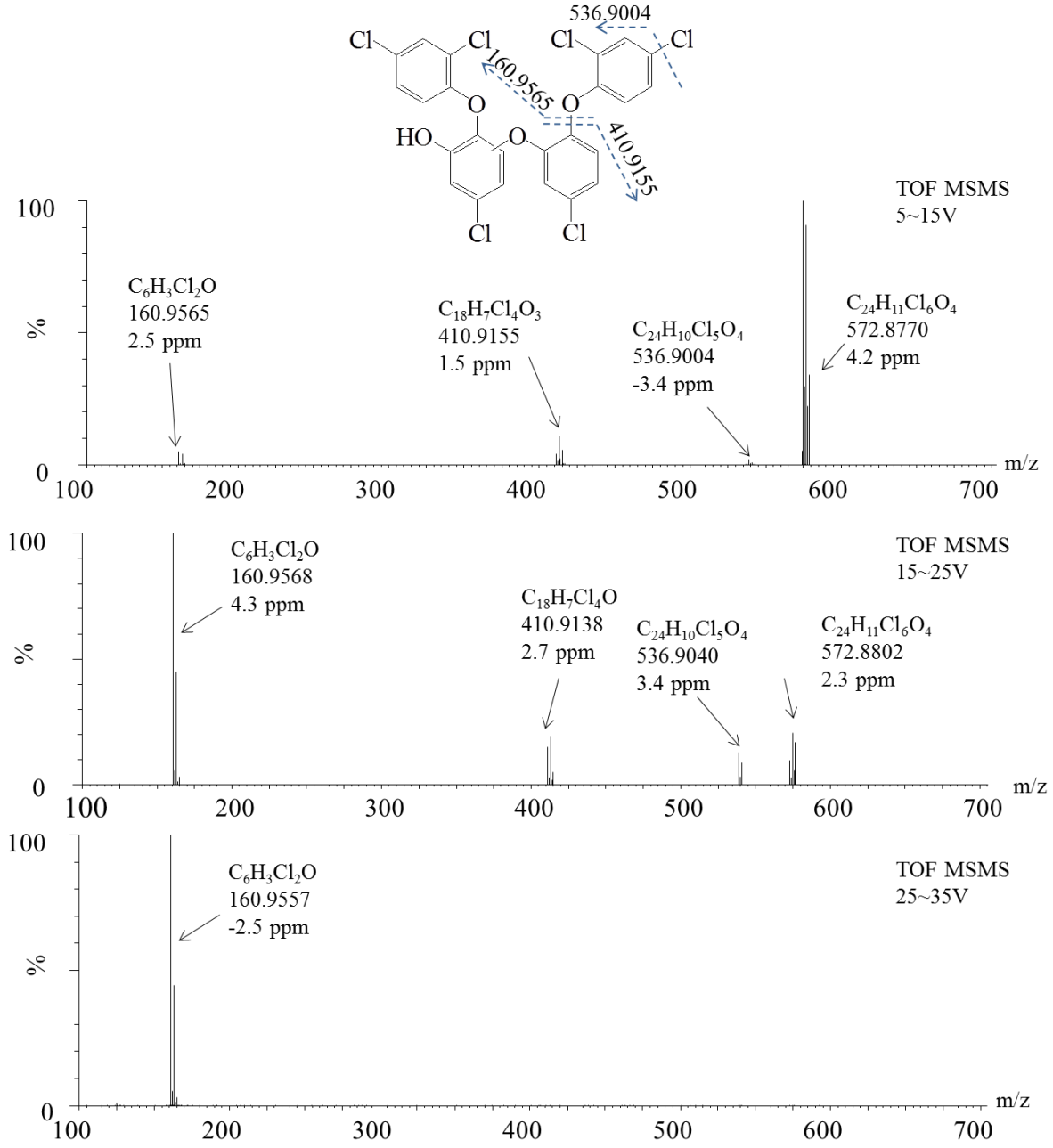

Fig. S2. MS/MS spectra under different collision energies and proposed structures of TCS-O-TCS.

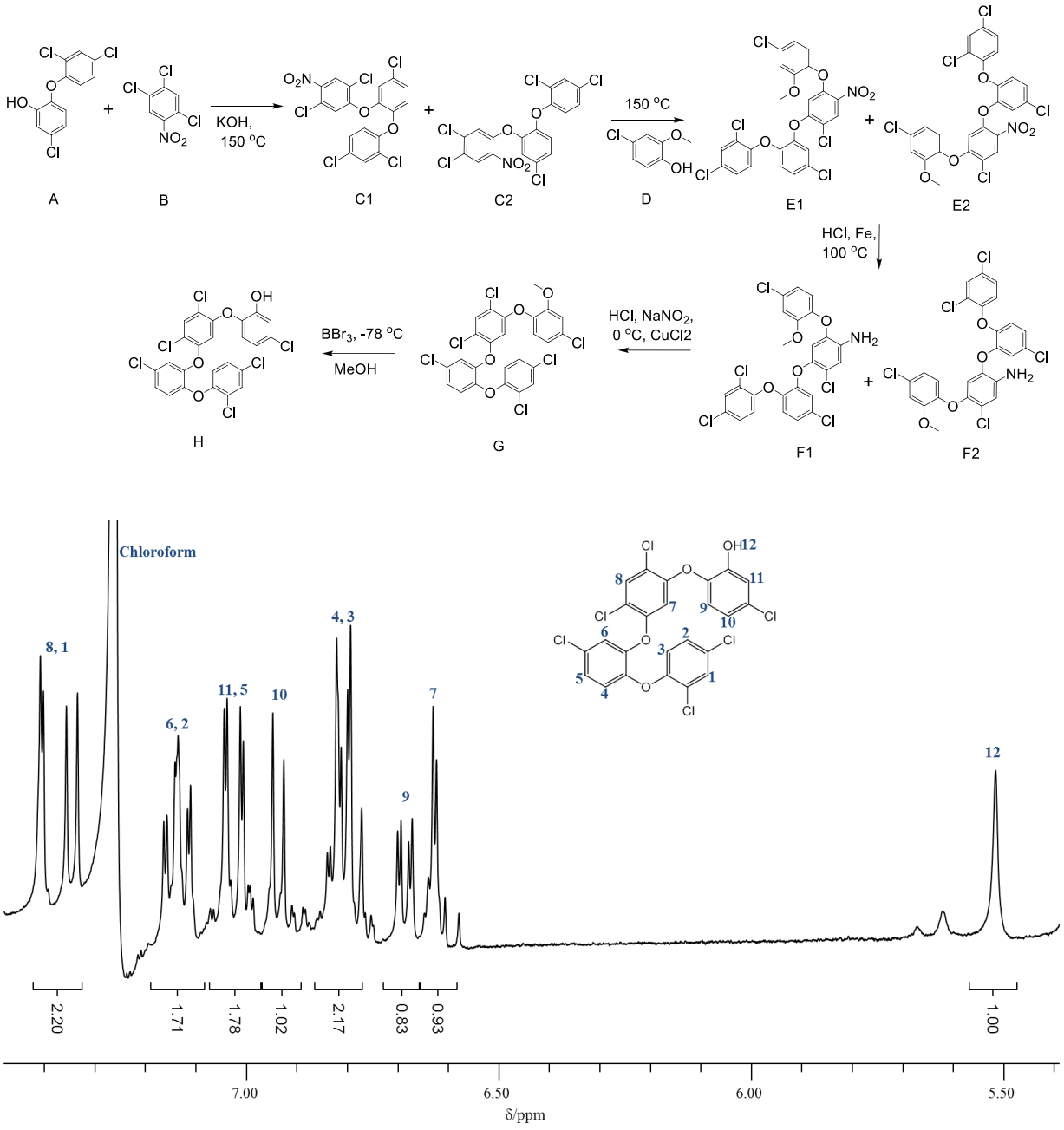

Fig. S3. Synthesis route of TCS-O-TCS (M6), and ^{1}H NMR spectrum (500 MHz, chloroform-d, p.p.m.) of the metabolite.

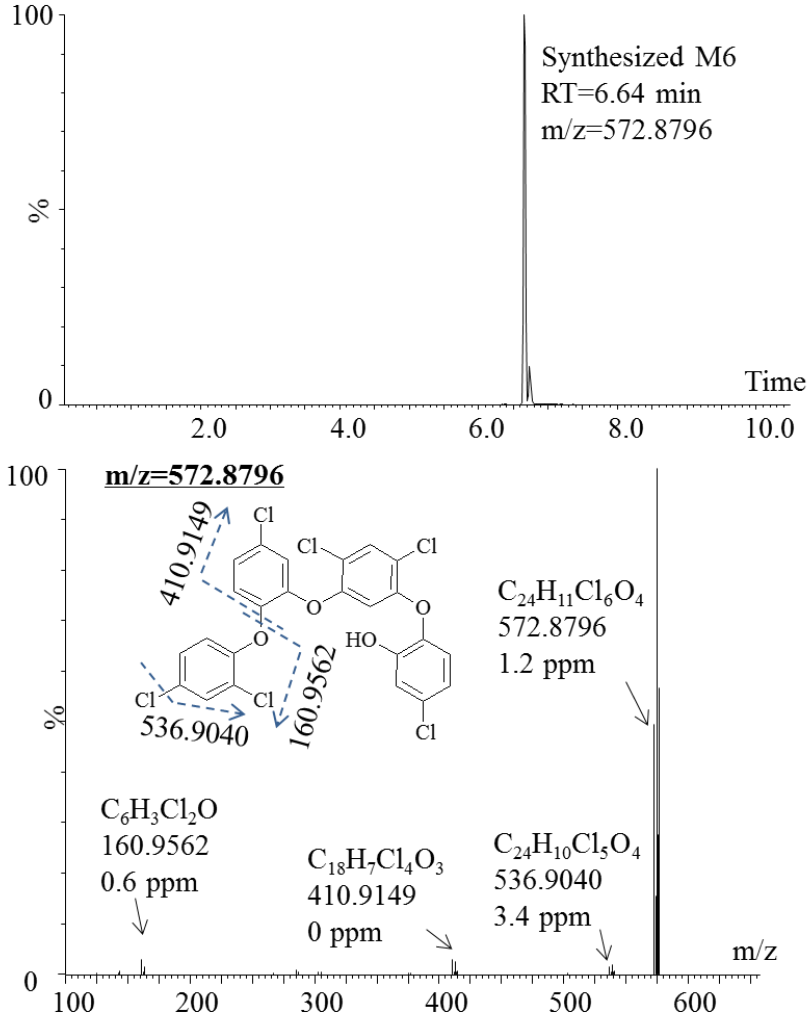

Fig. S4. Chromatogram and mass spectrum of synthesized TCS-O-TCS (M6).

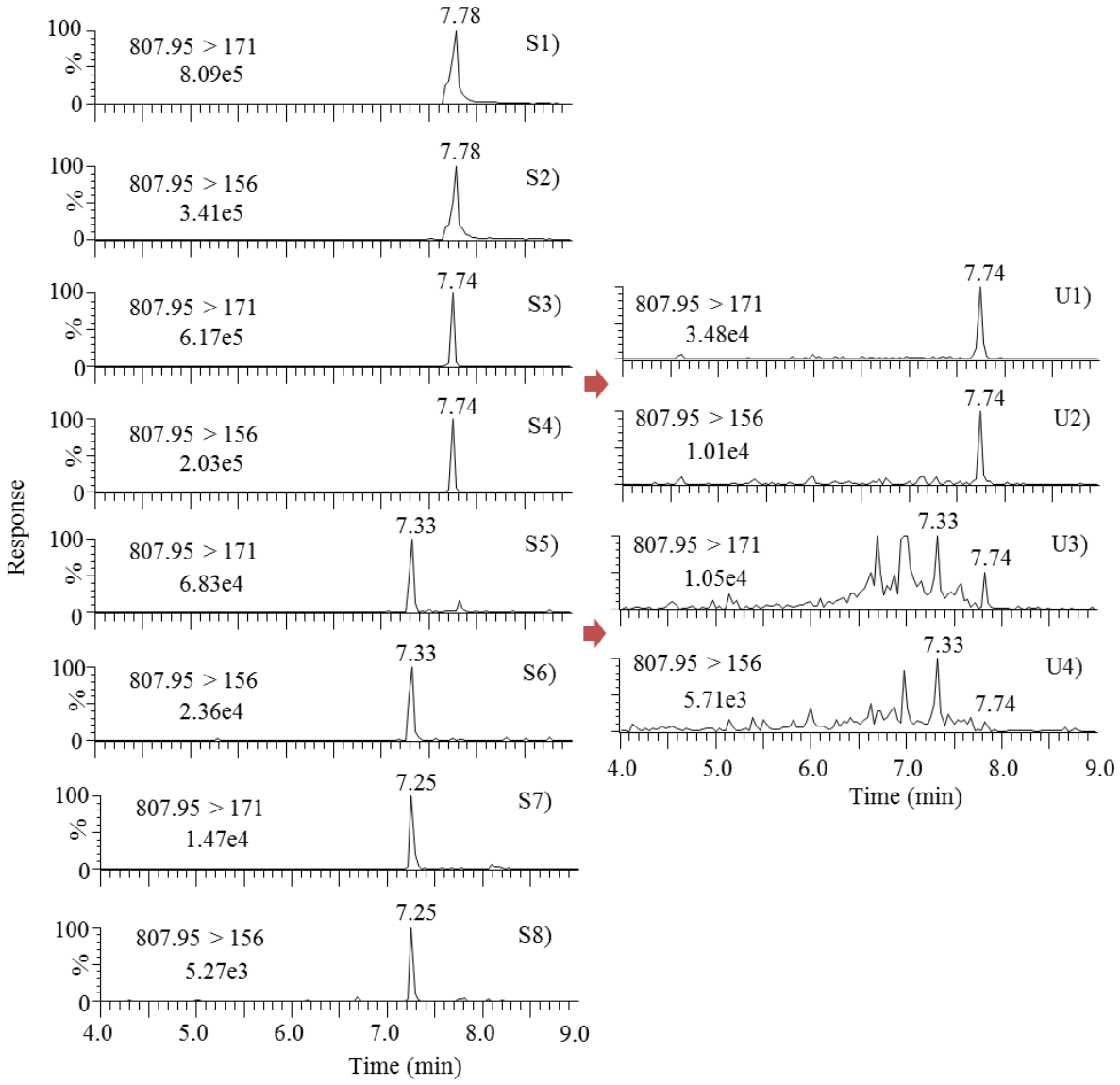

Fig. S5. Chromatogram of TCS-O-TCS derivertized with dansyl chloride (TCS-O-TCS-DNS) in separately purified TCS-O-TCS standards (S1-8) and extracts of urine samples (U1-4). Peaks showed in S1/2, S3/4, S5/6, and S7/8 were M7, M6, M3, and M2, respectively, and M4 and M5 cannot react with dansyl chloride. M6 (U1/2) and M3 (U3/4) were detected in the urine samples. Each TCS-O-TCS isomers were purified through preHPLC. The structure of the predominant metabolite (M6) was confirmed by chemically synthesized compound as shown in SI Appendix, Fig. S3.

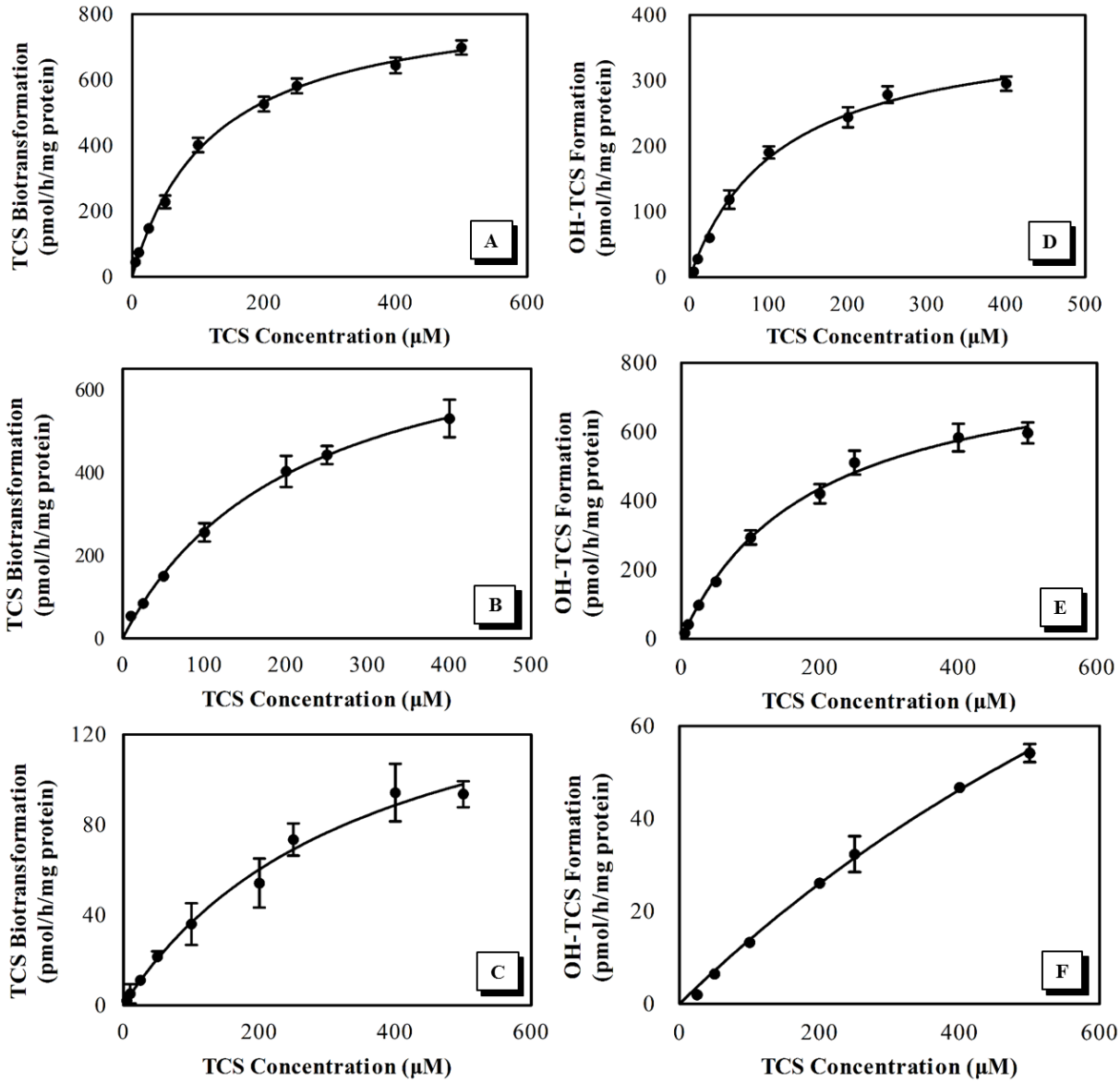

Fig. S6. Biotransformation kinetics of TCS in microsomes of human (A), quail (B) and weever (C), and formation kinetics of OH-TCS from TCS in microsomes of human (D), quail (E) and weever (F).

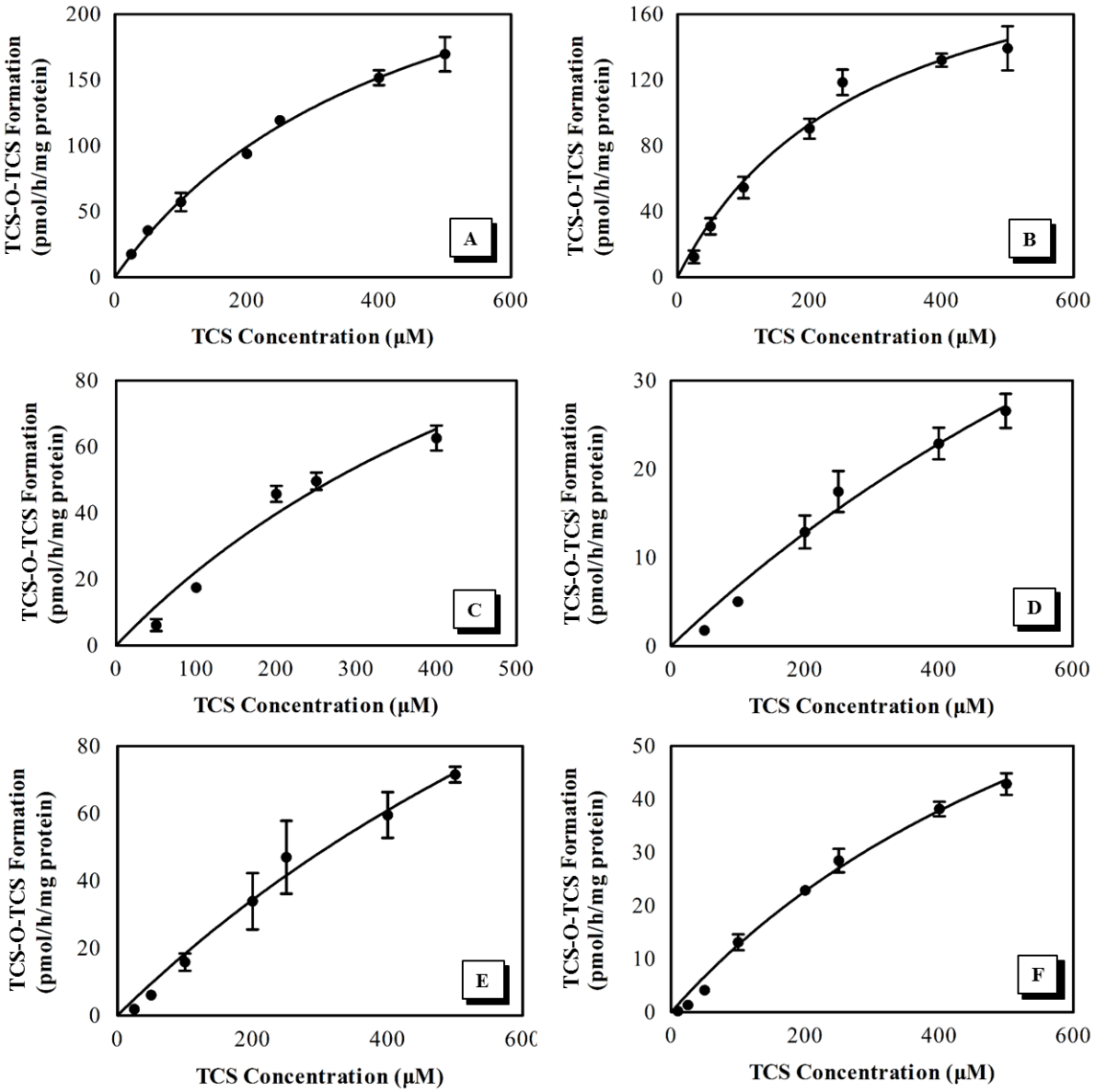

Fig. S7. Formation kinetics of two predominant TCS-O-TCS from TCS in microsomes of human (A, B), quail (C, D) and weever (E, F).

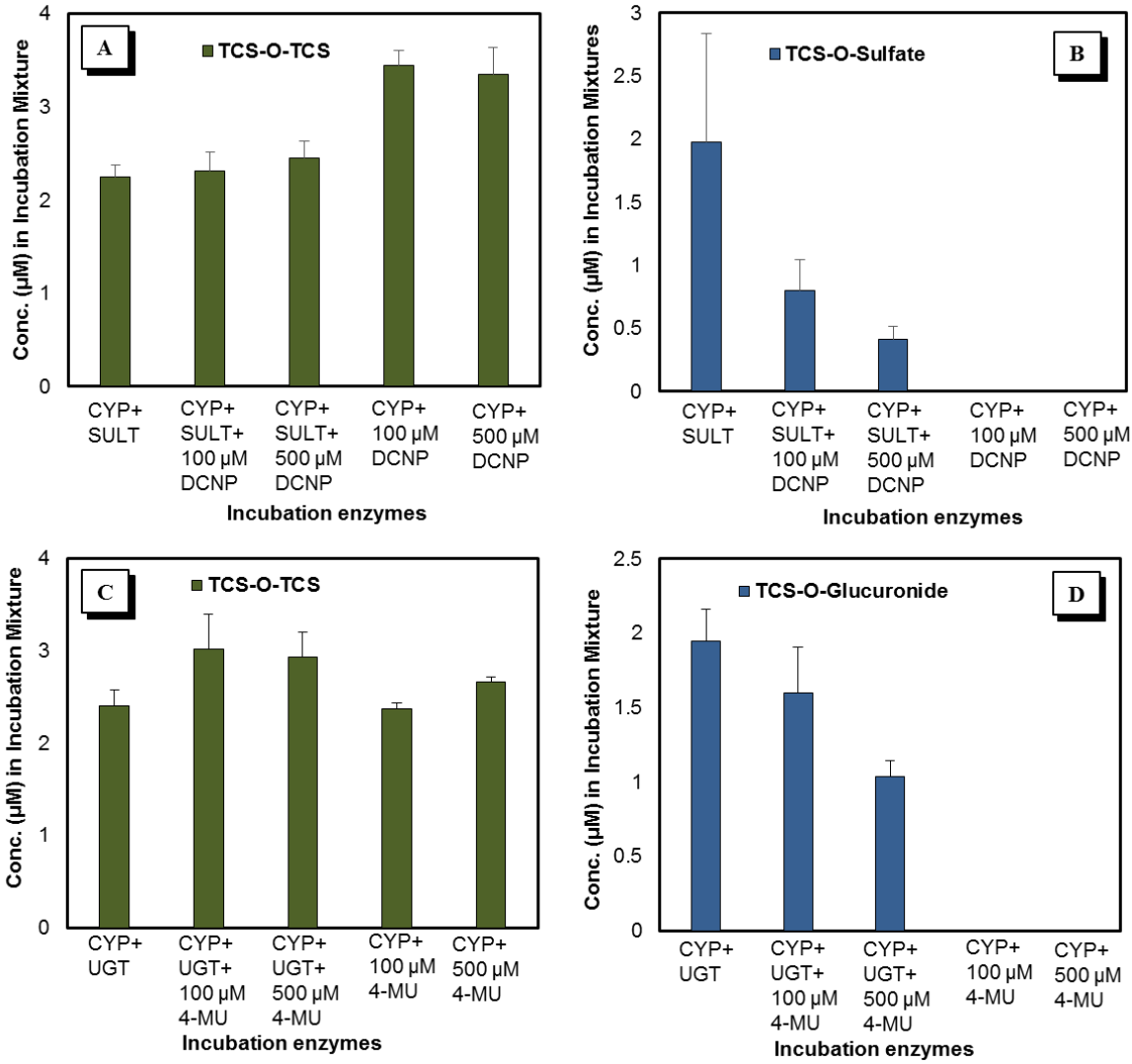

Fig. S8. Effects of SULT and UGT inhibitors (DCNP and 4-MU) on the concentrations of TCS-O-TCS, TCSO-Sulfate and TCS-O-Glucuronide after incubations in human microsomes. A) concentrations of TCS-O-TCS after incubation with phase I+II enzymes, phase I+II enzymes+DCNP, and phase I enzymes+DCNP; B) concentrations of TCSO-Sulfate after incubation with phase I+II enzymes, phase I+II enzymes+DCNP, and phase I enzymes+DCNP; C) concentrations of TCS-O-TCS after incubation with phase I+II enzymes, phase I+II enzymes+4-MU, and phase I enzymes+4-MU; D) concentrations of TCS-O-Glucuronide after incubation with phase I+II enzymes, phase I+II enzymes+4-MU, and phase I enzymes+4-MU.

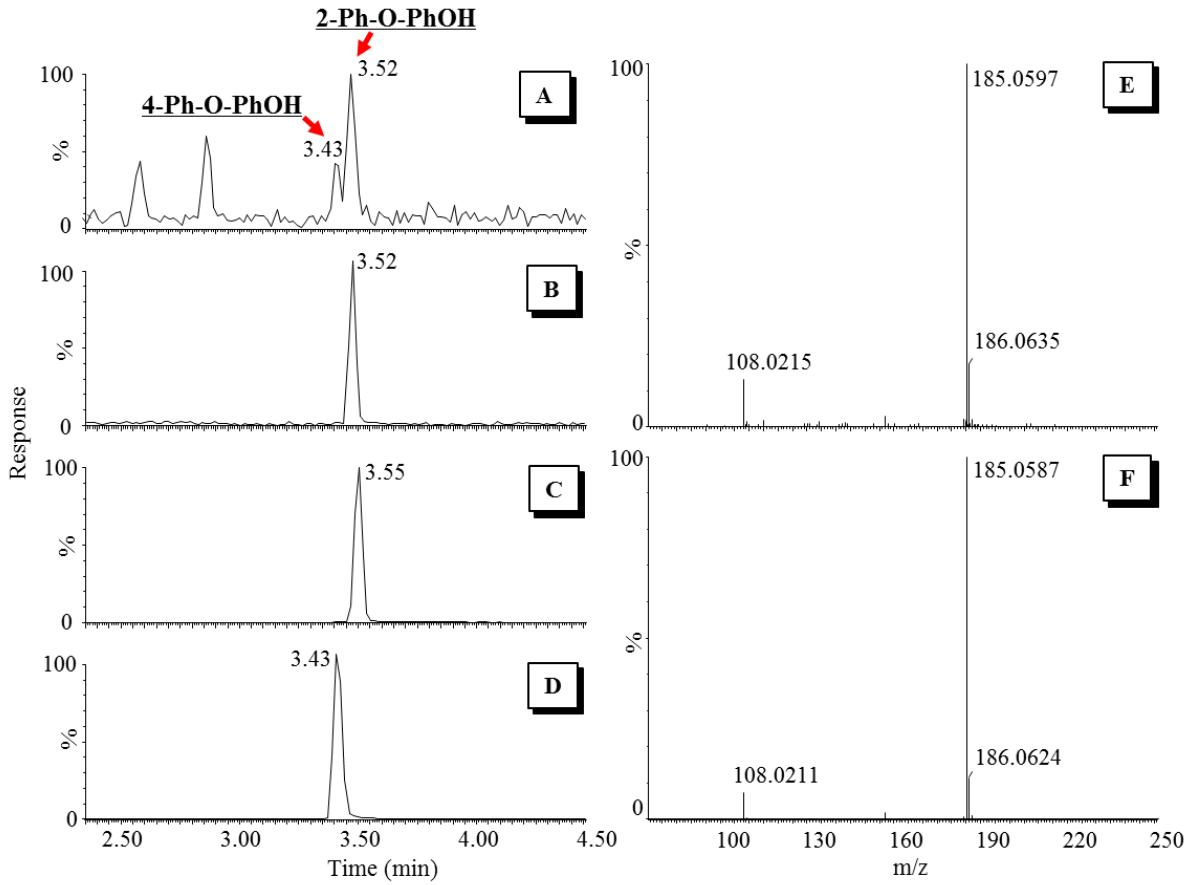

Fig. S9. Liquid chromatogram and QTOF mass spectra of the metabolic products of PhOH and standards of 2-Ph-O-PhOH, 3-Ph-O-PhOH, and 4-Ph-O-PhOH. A) chromatogram of the metabolic products of PhOH; B) chromatogram of 2-Ph-O-PhOH standard; C) chromatogram of 3-Ph-O-PhOH standard; D) chromatogram of 4-Ph-O-PhOH standard; E) mass spectrum of the peak at 3.52 min in incubation mixtures; F) mass spectrum of 2-Ph-O-PhOH.

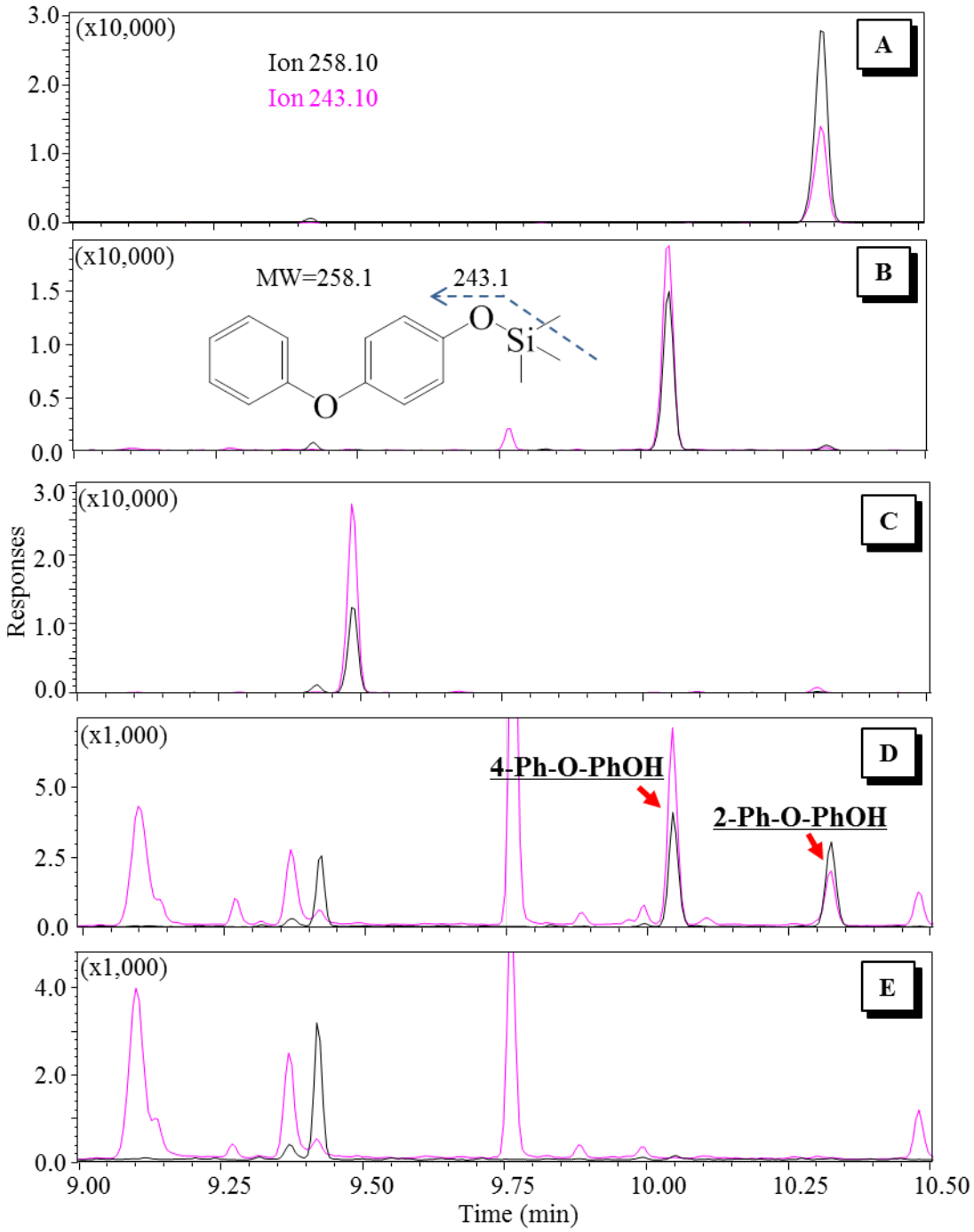

Fig. S10. GC-MS chromatogram of derivertized Ph-O-PhOH standards and the metabolic products of Ph. A) chromatogram of derivertized 2-Ph-O-PhOH standard; A) chromatogram of derivertized 4-Ph-O-PhOH standard; B) chromatogram of derivertized 3-Ph-O-PhOH standard; D) chromatogram of the metabolic products of Ph after incubation with liver microsomes; E) chromatogram of control samples after incubation with liver microsomes.

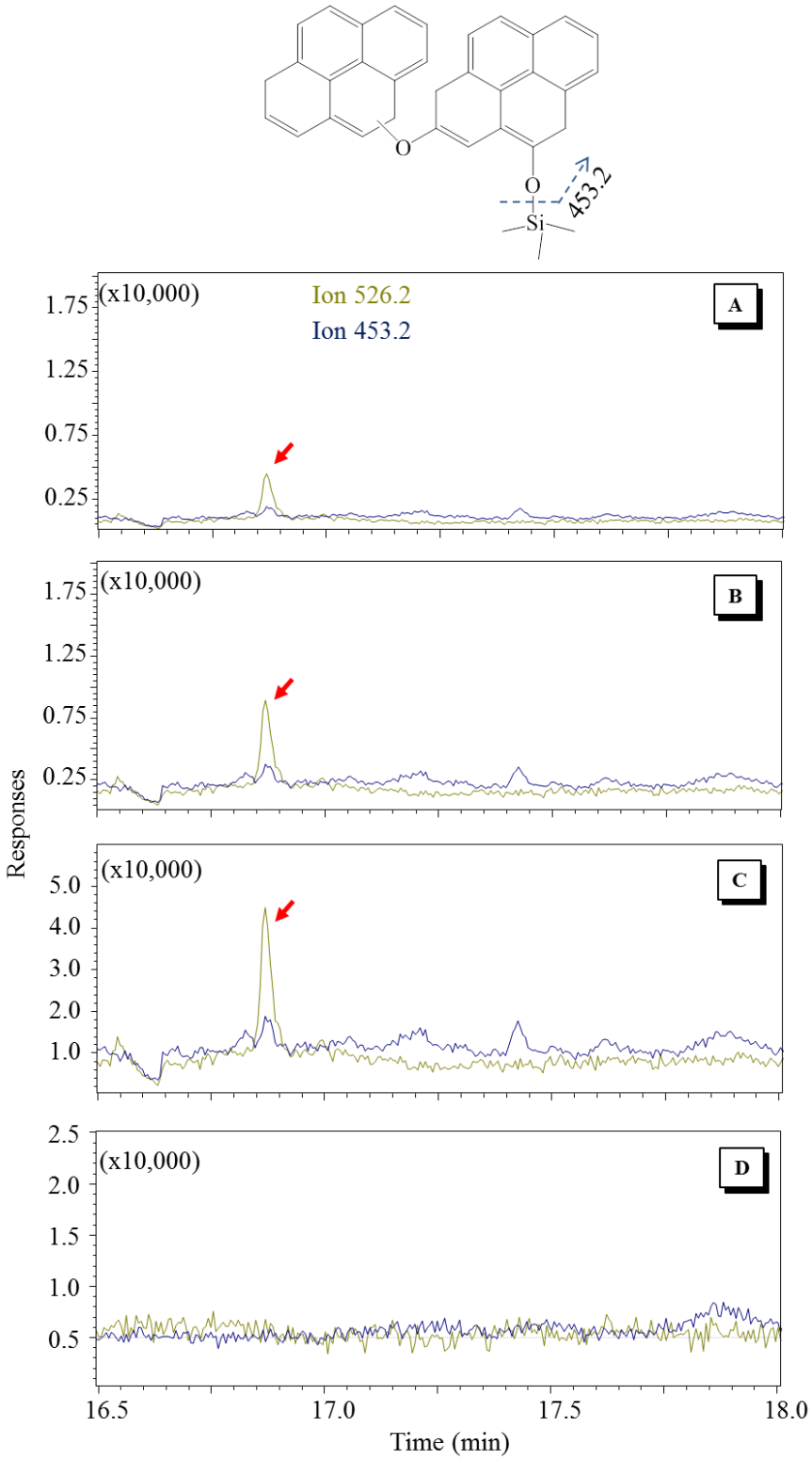

Fig. S11. GC-MS chromatograms of derivertized Py-O-PyOH when incubation concentrations of Py were 5 μM (A), 10 μM (B), 50 μM (C), and control samples (D) after incubation with liver microsomes.

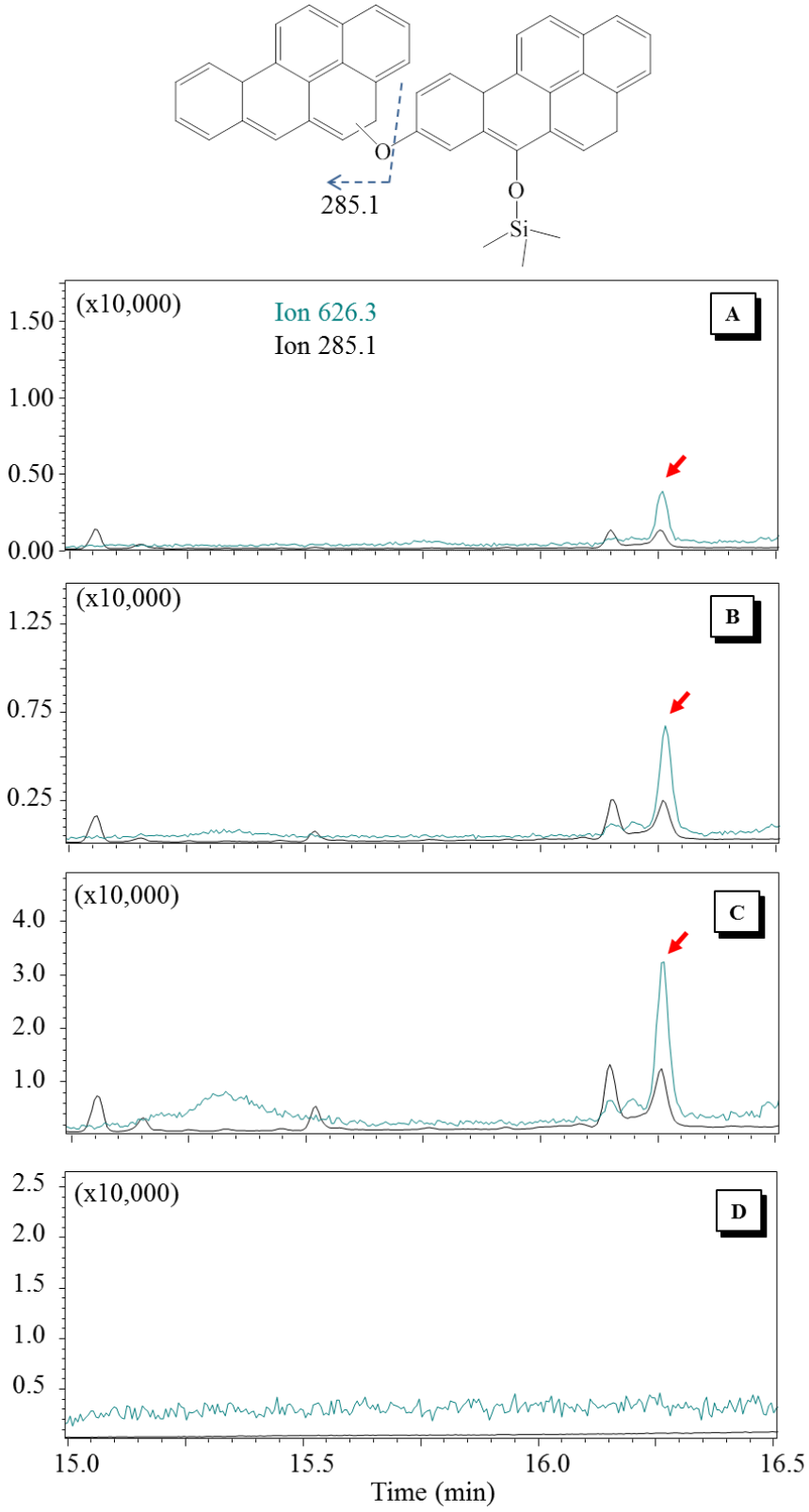

Fig. S12. GC-MS chromatograms of derivertized B[a]P-O-B[a]POH when incubation concentrations of B[a]P were 5 μM (A), 10 μM (B), 50 μM (C), and control samples (D) after incubation with liver microsomes.

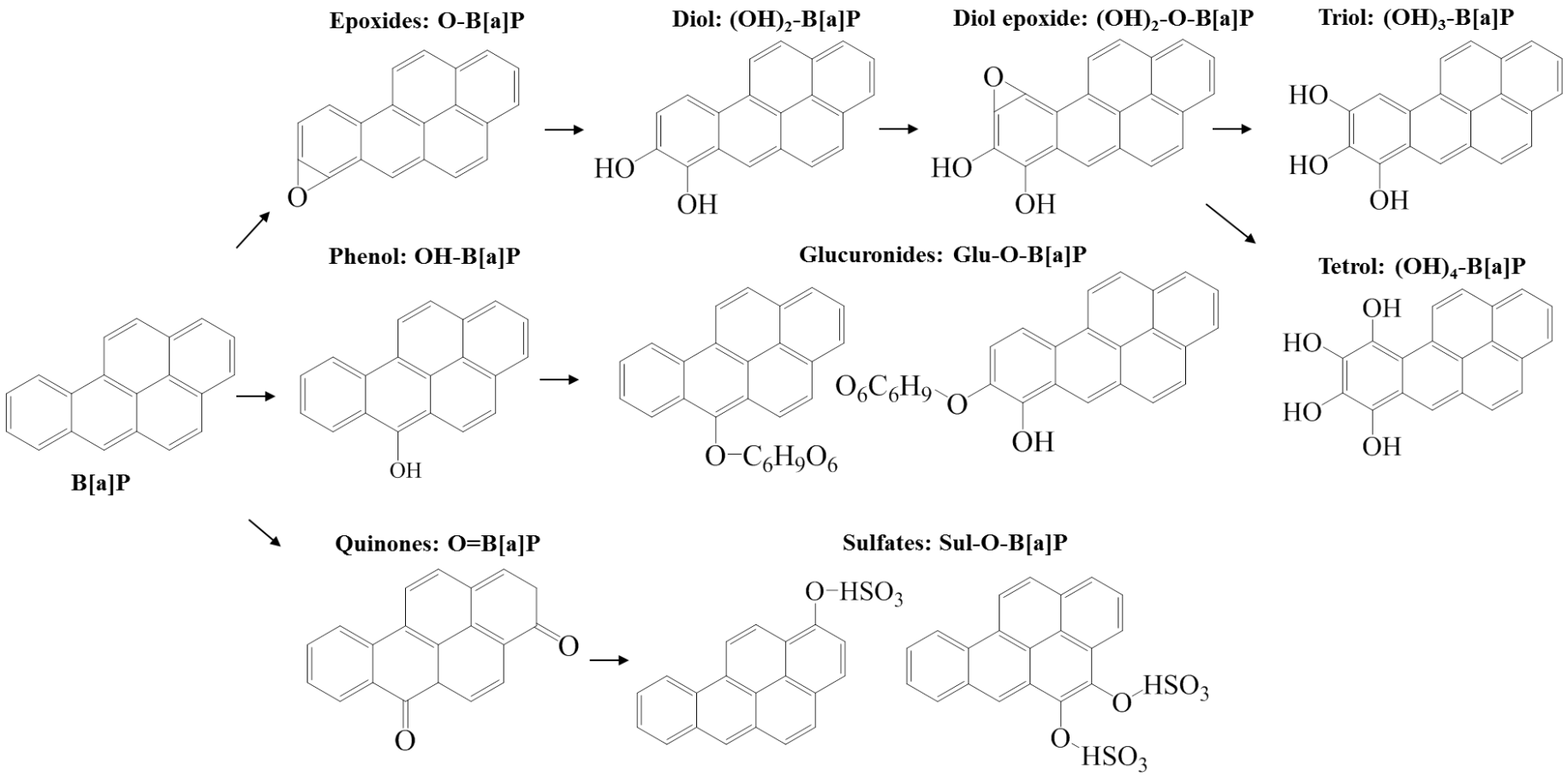

Fig. S13. Reported metabolic pathways of B[a]P.

Table S1. Characteristics of the population and concentrations of TCS and its biotransformation products in urine samples of the population.

Characteristic	Sample number
Enrolled	83
Age, year	31.2±4.9
BMI	22.1±3.3
Resident history, year	5±2.5
Sex, n (%)	
Male	48 (57.8)
Female	35 (42.2)
Smoking, n (%)	
Current smokers	16 (19.5)
Former smokers	7 (8.5)
Non-smokers	59 (72.0)
missing	1
Education, n (%)	
Primary school or below	1 (1.2)
Secondary school	13 (15.7)
High school	40 (48.2)
Bachelor degree	28 (33.7)
Master degree or above	1 (1.2)
Concentrations of TCS (ng/L)	
Geometric mean	11.9
Median	10.8
Maximum	190
Concentrations of TCS-O-TCS (ng/L)	
Geometric mean	0.19
Median	0.17
Maximum	47.9

Table S2. Kinetics of TCS and their biotransformation products in microsomes of various species.

Conditions	K_m (μM)	V_{max} (pmol/h/mg)	V_{max}/K_m (μL/h/mg)
TCS biotransformation			
Human microsomes	122.5±8.5	858.7±20.8	7
Quail microsomes	173.8±14.2	736.3±22.2	4.2
Fish microsomes	376.2±43.5	173.0±9.2	0.5
OH-TCS formation			
Human microsomes	114.2±12.7	390.1±16.5	3.4
Quail microsomes	189.3±18.7	847.3±34.6	4.5
Fish microsomes	1413±290.9	209.5±34.0	0.1
TCS-O-TCS formation			
Human microsomes	290.8~1154	103~1009	0.2~1.2
Quail microsomes	434.2~1931	35.3~837.9	0.1~0.4
Fish microsomes	795.4~1372	113.1~269.9	0.1~0.3

Table S3 Analytes and reaction monitoring conditions of derivertized TCS and TCS-O-TCS in UPLC-MS/MS analysis.

Analyte	MRM transition	Cone voltage (V)	Collision energy (eV)
TCS-DNS	523.74>171.0	50	31
	523.74>156.0	50	57
	523.74>114.6	50	70
TCS-O-TCS-DNS	807.95>171.0	50	31
	807.95>156.0	50	57
	809.94>171.0	50	31

Supporting Information references

1. Fan, Z. L., Hu, J. Y., An, W., Yang, M. (2013) Detection and occurrence of chlorinated byproducts of bisphenol A, nonylphenol, and estrogens in drinking water of China: comparison to the parent compounds. *Environ. Sci. Technol.* 47: 10841-10850.
2. Dyer, S.D., Bernhard, M.J., Cowan-Ellsberry, C. et al. (2009) In vitro biotransformation of surfactants in fish. Part II - Alcohol ethoxylate (C16EO8) and alcohol ethoxylate sulfate (C14EO2S) to estimate bioconcentration potential. *Chemosphere* 76: 989-998.
3. Diaz, G. J.; Murcia, H. W.; Cepeda, S. M. (2010) Cytochrome P450 enzymes involved in the metabolism of aflatoxin B1 in chickens and quail. *Poult. Sci.* 89: 2461-2469.
4. Bradford M M. (1976) A rapid and sensitive method for the quantitation of microgram quantities of protein utilizing the principle of protein-dye binding. *Analytical biochemistry* 172(1): 248-254.